Multi-Directional Continuous Traffic Model For Large-Scale Urban Networks

Liudmila Tumash, Carlos Canudas de Wit, Maria Laura Delle Monache

Multi-Directional Continuous Traffic Model For Large-Scale Urban Networks

Liudmila Tumash[a], Carlos Canudas-de-Wit[a], Maria Laura Delle Monache[b,*]

[a] *Univ. Grenoble Alpes, CNRS, Inria, Grenoble INP, GIPSA-Lab, France*
[b] *University of California, Berkeley, USA*

Abstract

In this paper, we propose a new multi-directional two-dimensional continuous model for urban traffic. It is called the NEWS model, since it represents a system of four partial differential equations (PDEs) that describe propagation of vehicle density in cardinal direction layers: North, South, West and East. The NEWS model can be applied to predict traffic evolution on a general urban network of arbitrary size by knowing only its boundary flows, as well as its topology and infrastructure parameters such as roads speed limits, number of lanes and capacities. The flux direction is retrieved from turning ratios at intersections, which is then aggregated in four direction layers using geometrical projection matrices. We show its formal derivation step-by-step from the classical Cell Transmission Model at one intersection. We then show that the NEWS model is a hyperbolic PDE system that corresponds to a conservation law with bounded densities. The model prediction performance is validated using synthetic data from the microsimulator Aimsun. Finally, the model is also validated using real data collected from a network of sensors installed in Grenoble (a city in France).

Keywords: Macroscopic model for urban traffic, partial differential equations, simulation and validation, continuation of ODE to PDE, conservation laws.

*Corresponding author
Email addresses: liudmila.tumash@gipsa-lab.fr (Liudmila Tumash), carlos.canudas-de-wit@gipsa-lab.grenoble-inp.fr (Carlos Canudas-de-Wit), mldellemonache@berkeley.edu (Maria Laura Delle Monache)

1. Introduction

The development of traffic models based on the conservation principle has been mostly influenced by the Lighthill-Whitham-Richards model (LWR) proposed in the fifties by [1] and [2]. This model is the most simple and therefore the most popular macroscopic model for traffic. The LWR model represents the kinematic wave theory for traffic, i.e., it describes temporal evolution of vehicle density ρ on a single highway road of infinite length as if it were a compressible fluid. Mathematically, the LWR model is a first-order scalar hyperbolic partial differential equation

$$\partial_t \rho(x,t) + \partial_x \Phi(\rho) = 0, \qquad \forall (x,t) \in \mathbb{R} \times \mathbb{R}^+,$$

where $\Phi(\rho)$ is a concave flow-density relation. This relation represents an empirically measured law known as the fundamental diagram (FD), which was first formalized in [3]. Despite the appearance of more sophisticated and even higher-order macroscopic models (see [4] for a review), the LWR model remains the most popular one due to its simplicity and ability to reproduce the most essential traffic phenomena such as wave formation and propagation.

Although being a simple model, the analysis of its solution is a tedious task. In general, nonlinearity of FD introduces nonlinearities in the characteristic fields of LWR PDE. Therefore, even with a smooth initial datum characteristic lines may intersect, which leads to discontinuities at intersection points. Whenever this happens, the conservation law solution is not defined in the classical sense and needs to be considered in its weak formulation. This formulation yields multiple solutions, among which the entropy solution [5] is recognized to be the physically reasonable one. Properties of hyperbolic conservation laws were extensively studied, see [6, 7, 8].

There is however a way to study kinematic waves of traffic without any need to deal with solution shocks. In [9, 10, 11] Newell proposed an alternative way to consider traffic on a macroscopic scale by numbering vehicles at a highway entry and following the evolution of vehicle numbers at every location and time,

i.e., traffic state can be described in terms of cumulative number of vehicles. Its dynamics are governed by a Hamilton-Jacobi PDE, which represents an integral form of the LWR PDE. Its solution is a Lipschitz continuous function that is free of shocks and can obtained by solving a simple minimization problem.

A variational formulation of kinematic waves was studied in [12, 13], who showed that every well-posed traffic problem with a concave flow-density relation can be solved as a set of shortest paths. In general, the explicit solution of Hamilton-Jacobi PDE can be obtained using the viability framework, which was first shown for the case of convex conservation laws in [14, 15]. The viability framework is based on Lax-Hopf formula that exploits the structure of a dynamic programming problem, and the solution is obtained as the minimum of all valid paths, see [16]. Several computational algorithms were developped to obtain solutions of Hamilton-Jacobi PDE in the context of traffic, e.g., [17] computes a solution for any piecewise affine initial condition. The Lax-Hopf algorithm to compute a solution for any concave FD has been suggested by [18], and its improved version with a lower computational time has been proposed in [19].

In some cases, the exact solution to LWR PDE can be obtained using the wave-front tracking method [20, 21]. The solution of LWR PDE can also be numerically approximated using computational methods such as the Godunov scheme [22] or Lax-Friedrichs method [23]. These are both finite difference methods. The Godunov scheme deals with Riemann problems at each cell, and the Lax-Friedrichs method requires adding artificial viscosity.

A time-discrete approximation of the LWR equation was introduced in [24, 25], which is now known as the Cell Transmission Model (CTM). This model can be viewed as a Godunov-type discretization of LWR, and it is based on approximating links (roads) by cells. The amount of flux transmitted between cells is based on their current occupancy (the demand-supply concept). Later, [26] proposed the Link Transmission Model (LTM) based on the cumulative number of vehicles, i.e., LTM can be seen as discretization of the variational formulation of LWR. Both discrete models (CTM and LTM) are very popular due to their simplicity and the ability of a straightforward extension to networks.

In its original formulation, the LWR model is applicable only to single roads of infinite length. Extension to urban networks required developing a methodology for intersection modeling within the LWR framework. This was first done at the end of the last century by [27] who considered a network of uni-directional roads. Later on, this formulation was refined to capture multi-directional traffic, e.g. see [28]. The CTM has also been extended to networks in [25], who considered networks as directed graphs consisting of links (roads) and nodes (junctions). The general theory of traffic flow on networks is presented in [29]. Recently, the variational theory of traffic flow has also been extended to networks in [30]. However, although being quite accurate, network-based traffic modeling might become a tedious task when it comes to large networks containing thousands of roads due to a high computational cost, which is determined by the number of roads and junctions in a network [31]. Moreover, network-based formulation of traffic requires considering thousands of equations (in case of large networks), which exaggerates any explicit analysis of system properties or control design.

Another way to describe the evolution of urban traffic, that is more suitable for explicit analysis, is to use dynamic two-dimensional continuum models. These share a lot of features with pedestrian models [32] with the difference that, unlike pedestrian crowds, vehicles are restricted to move on roads. In [33] authors considered a model including a diffusion term and a drift term that depends on the density. The direction of the drift vector is determined by the shape of the network. Other works [34, 35, 36] define the flux function by solving Eikonal equations such that traffic flow takes the path of the lowest cost. For a review of 2D continuum models the reader is referred to [37]. A recent work [38] introduced a direct extension of LWR model in two dimensions:

$$\frac{\partial \rho(x,y,t)}{\partial t} + \nabla \cdot \vec{\Phi}(x,y,\rho) = 0, \qquad \forall (x,y,t) \in \mathbb{R}^2 \times \mathbb{R}^+.$$

Thereby, the flux function became a vector. Its direction is retrieved from the geometry of the underlying urban network, while the flux magnitude depends on network infrastructure parameters that are incorporated into the space-

dependency of the fundamental diagram.

The aforementioned references however consider traffic flow that has only one direction of motion. The first attempt to include multiple directions in 2D continuum models was made only several years ago, when [39] took inspiration from pedestrian modeling and deployed dynamic user-optimal principle for the path choice. The drawback of this model is that the traffic density may become unbounded (it is not based on a fundamental diagram). There exist also other works [40, 41] proposing 2D multi-layer models with bounded densities. However, they do not include mixing between different direction layers, i.e., vehicles can not change their direction of motion. These models are also not necessarily hyperbolic, i.e., their PDE type varies with parameters, which exaggerates its analysis and numerical simulation. Hyperbolicity for all parameters implies that it can be analysed like many other conservation law based models for traffic.

Contribution. We fix both of these aspects (lack of PDE type and unbounded densities) and provide a formal derivation of a new 2D macroscopic model describing traffic propagation in a general urban network of arbitrary size. The resulting NEWS model is a conservation law that represents a hyperbolic PDE system with bounded densities in each layer. This model can be seen as an **extension of classical LWR to general urban networks**. The main novelty of our model compared to other PDE-based 2D traffic models is that it includes mixing between different density layers, i.e., it allows cars to change their original direction of movement (capturing the origin-destination concept). Such a PDE model can then be used for explicit analysis or control design by analysing a system that consists only of four equations. Also unlike [40], the NEWS model can be applied to any kind of sparse urban networks, since it treats densities in a 1D sense, and therefore does not rely on the assumption that a urban network is dense enough to be approximated as a continuum. A simple control for congested traffic with NEWS-governed dynamics has already been presented in [42].

The structure of this paper is the following. In Section 2, we state the main result of this paper, which is the NEWS model. Then, in Section 3 we review

the CTM for one intersection, thereby introducing several important concepts (e.g., partial flows and supply ratios) that complete the description of the multi-directional nature of traffic. The NEWS formalism that introduces geometrical projections of flows on roads into cardinal directions is presented in Section 4. The NEWS model is derived from the CTM in Section 5, where we also show how to obtain a PDE from an ODE (ordinary differential equation) using a new continuation method presented in [43]. In Section 6, mathematical properties of the NEWS model are analysed: the conservation law property, hyperbolicity and boundedness of its state (four-dimensional density). In Section 7, we provide a numerical example verifying the ability of the model to predict traffic evolution in Grenoble downtown using synthetic and real sensor data. Finally, the concluding remarks are given in Section 8.

2. Main result

This paper is devoted to a step-by-step derivation of the continuous PDE-based model of a general traffic network in some urban area. In this section we directly state the resulting model and then introduce the derivation workflow that summarizes the rest of the paper devoted to the model derivation and validation.

The full NEWS model is given by the following set of four partial differential equations defined at each point (x, y) in some continuum urban area:

$$\begin{cases} \dfrac{\partial \bar{\rho}_N}{\partial t} = \dfrac{1}{L}\left(\bar{\phi}_N^{in} - \bar{\phi}_N^{out}\right) - \dfrac{\partial(\overline{\cos\theta}_N \bar{\phi}_N)}{\partial x} - \dfrac{\partial(\overline{\sin\theta}_N \bar{\phi}_N)}{\partial y}, \\ \dfrac{\partial \bar{\rho}_E}{\partial t} = \dfrac{1}{L}\left(\bar{\phi}_E^{in} - \bar{\phi}_E^{out}\right) - \dfrac{\partial(\overline{\cos\theta}_E \bar{\phi}_E)}{\partial x} - \dfrac{\partial(\overline{\sin\theta}_E \bar{\phi}_E)}{\partial y}, \\ \dfrac{\partial \bar{\rho}_W}{\partial t} = \dfrac{1}{L}\left(\bar{\phi}_W^{in} - \bar{\phi}_W^{out}\right) - \dfrac{\partial(\overline{\cos\theta}_W \bar{\phi}_W)}{\partial x} - \dfrac{\partial(\overline{\sin\theta}_W \bar{\phi}_W)}{\partial y}, \\ \dfrac{\partial \bar{\rho}_S}{\partial t} = \underbrace{\dfrac{1}{L}\left(\bar{\phi}_S^{in} - \bar{\phi}_S^{out}\right)}_{\text{mixing term}} - \underbrace{\dfrac{\partial(\overline{\cos\theta}_S \bar{\phi}_S)}{\partial x} - \dfrac{\partial(\overline{\sin\theta}_S \bar{\phi}_S)}{\partial y}}_{\text{transportation term}}. \end{cases}$$

The state of this model is given by the four-dimensional vector $\bar{\rho} = \bar{\rho}(x, y, t) = (\bar{\rho}_N, \bar{\rho}_E, \bar{\rho}_W, \bar{\rho}_S)$, representing densities of the traffic flows in four cardinal directions. Functions $\bar{\phi}$, $\bar{\phi}_{in}$ and $\bar{\phi}_{out}$ are defined via fundamental diagrams and

are space- and state-dependent. Finally, L, $\overline{\cos\theta}$ and $\overline{\sin\theta}$ are *space-dependent* (but not state-dependent or time-dependent) parameters which represent the topology of the particular traffic network.

The right-hand side of the model consists of two parts: mixing term and transportation term. The mixing term accounts for the coupling between traffic flows in different direction layers. The transportation term consists of spatial derivatives, and therefore describes the transportation of traffic density in the same way as it is done in the original LWR model. Therefore, the NEWS model can be seen as a **continuous generalisation of LWR to a 2-dimensional multi-directional urban traffic networks**. This simple analytic representation of urban traffic can facilitate the analysis for explicit control design.

In the following sections we will formally derive this model starting from the CTM on intersections. The workflow diagram explaining the derivation process is presented in Fig. 1.

3. Traffic model for one intersection

LWR model in its original form (single highway roads) is the most simple macroscopic model, which however reflects the most important traffic phenomena such as wave formation and propagation. Therefore, we use the CTM (discretized version of LWR) at one intersection as a starting point. Thereby, we will define several important variables that will be later used to derive a continuous PDE-based model for the whole network.

Let us consider an intersection located at (x_1, y_1) with two incoming and two outgoing roads (as illustrated in Fig. 2), and show a step-by-step derivation of the traffic model at this intersection. Then, the traffic model will be generalized for an intersection with an arbitrary number of roads.

3.1. Demand-supply concept

One of the key assumptions in traffic modeling is that there is a concave relation between traffic flow ϕ and vehicle density ρ. This relation is an empirical

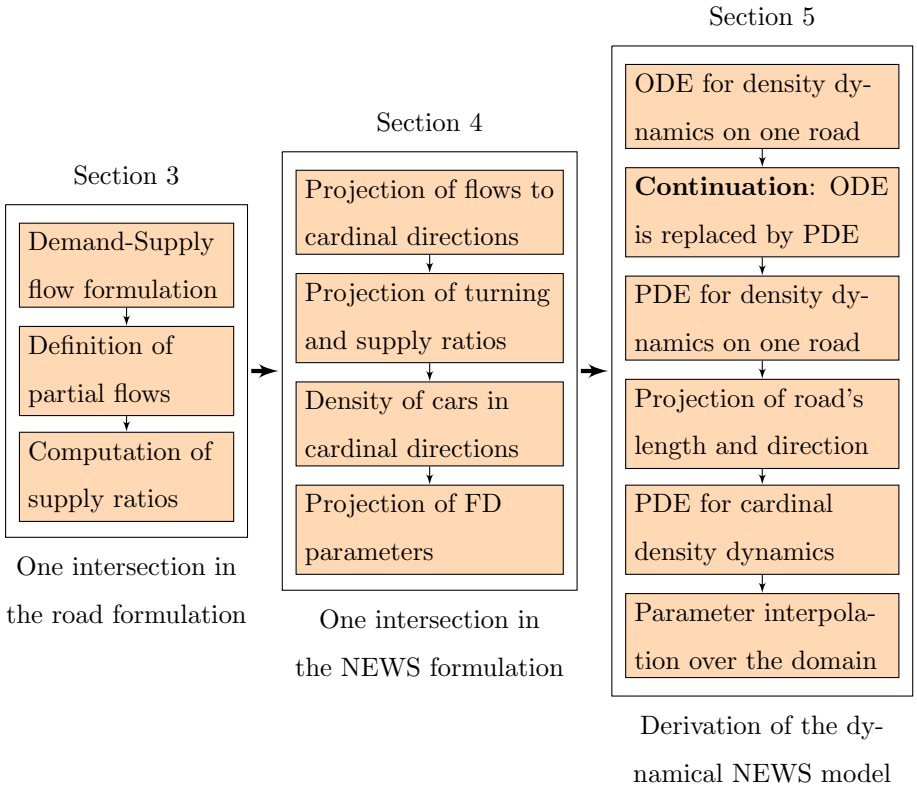

Figure 1: Workflow diagram of the derivation of the NEWS model.

law known as the fundamental diagram (FD) [3]. Mathematically, FD $\Phi(\rho) : [0, \rho_{max}] \to \mathbb{R}^+$ is a concave function with a unique maximum ϕ_{max} (road *capacity*) achieved at the *critical density* ρ_c, while the minimum is achieved at $\Phi(0) = \Phi(\rho_{max}) = 0$, i.e., for zero and *maximal density* ρ_{max} (also called the traffic jam density). If traffic density is below its critical value ρ_c, then vehicles move in a **free-flow regime** with a *positive kinematic wave speed* v, otherwise they move in a **congested regime** characterized by a *negative kinematic wave speed* ω. Notice that the fundamental diagram parameters such as speed limits, capacities and maximal densities might vary from road to road.

Consider a road divided into two cells as illustrated in Fig. 3. In accordance

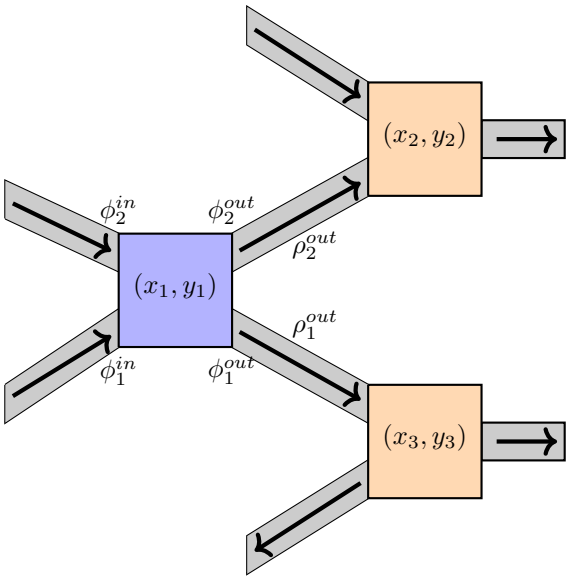

Figure 2: Example of a small traffic network consisting of 3 intersections. We consider the intersection filled in blue.

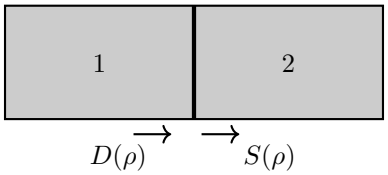

Figure 3: Schematic illustration of demand-supply concept.

with the demand-supply concept introduced in [24, 25], the amount of flux transmitted between cells is determined by the minimum between demand $D(\rho)$ of cell 1 and supply $S(\rho)$ of section 2:

$$\phi(\rho) = \min\left\{D(\rho), S(\rho)\right\}, \quad \forall t \in \mathbb{R}^+, \tag{1}$$

where $D(\rho)$ and $S(\rho)$ are defined as

$$D(\rho) = \begin{cases} \Phi(\rho), & \text{if} \quad 0 \leq \rho \leq \rho_c, \\ \phi_{max}, & \text{if} \quad \rho_c < \rho \leq \rho_{max} \end{cases} \tag{2}$$

and

$$S(\rho) = \begin{cases} \phi_{max}, & \text{if} \quad 0 \leq \rho \leq \rho_c, \\ \Phi(\rho), & \text{if} \quad \rho_c < \rho \leq \rho_{max}. \end{cases} \tag{3}$$

The demand-supply concept represents the key element of Cell Transmission Model that is a time-discrete approximation of kinematic wave model (LWR).

3.2. Flows at intersections: example

We use the demand-supply concept to derive a traffic flow model for the intersection at (x_1, y_1) as illustrated in Fig. 2. In particular, we need to determine inflows $\phi^{in}(t)$ and outflows $\phi^{out}(t)$ for this intersection, which stay in balance

$$\phi_1^{in} + \phi_2^{in} = \phi_1^{out} + \phi_2^{out}.$$

Note that throughout this paper, we use a subscript to number roads, and a superscript is used to indicate whether this particular road is incoming or outgoing, e.g., $\phi^{in}_{max,1}$ is the capacity of incoming road number 1.

Let us now assume that the fundamental diagram has a *triangular* shape as in [24]. In this case, the demand and supply functions from (2) and (3) become:

$$D(\rho) = \min\left\{v\rho, \phi_{max}\right\}, \quad S(\rho) = \min\left\{\omega(\rho_{max} - \rho), \phi_{max}\right\}. \tag{4}$$

Thereby, the values of traffic jam ρ_{max} and critical densities ρ_c are the same for every road, and they depend only on the minimal headway distance between vehicles, which is a function of cultural driving habits and the average vehicle length. In contrast, the values of the kinematic wave speeds v and ω vary form one road to another, since these are related to the speed limits, the ratio of green to red traffic signals and the presence of bottlenecks.

Remark 1. Notice that, in general, the derivation of the model relies only on the demand-supply concept, which is applicable also for a more general FD shape (not only triangular) as long as it is a concave function of density. We assumed the triangular shape only to gain more clarity during the upcoming step-by-step model derivation.

Each incoming road has its own flow demand to enter the intersection (illustrated in Fig. 2) that reads with (4):

$$D_1 = \min\left\{v_1^{in}\rho_1^{in}, \phi_{max,1}^{in}\right\}, \quad D_2 = \min\left\{v_2^{in}\rho_2^{in}, \phi_{max,2}^{in}\right\}. \tag{5}$$

A part of the flow entering the intersection goes to the first outgoing road and the other part goes to the second outgoing road. These flows are split according to the *turning ratios* (TR) $\alpha_{ij} \in [0,1]$, where i is the index of the incoming road and j is the index of the outgoing road. For instance, if $\alpha_{11} = 0.6$ and $\alpha_{12} = 0.4$, then 60% of vehicles from the first incoming road turn to the first outgoing road, and 40% turn to the second outgoing road. Note also that the sum of turning ratios for each incoming road must be 1, i.e.,

$$\alpha_{11} + \alpha_{12} = 1, \quad \alpha_{21} + \alpha_{22} = 1.$$

The concept of TR was discussed, for example, in [25] for the case of diverging intersections. Notice that turning ratios can be measured by collecting data of origin and destination of vehicles.

Let us now introduce the concept of **partial demands**. A partial demand refers to demand flow of an incoming road to enter a *particular* outgoing road. These are equal to the overall demands (5) multiplied by corresponding TR:

$$\begin{aligned} D_{11} &= \min\left\{\alpha_{11}v_1^{in}\rho_1^{in}, \alpha_{11}\phi_{max,1}^{in}\right\}, \quad D_{12} = \min\left\{\alpha_{12}v_1^{in}\rho_1^{in}, \alpha_{12}\phi_{max,1}^{in}\right\}, \\ D_{21} &= \min\left\{\alpha_{21}v_2^{in}\rho_2^{in}, \alpha_{21}\phi_{max,2}^{in}\right\}, \quad D_{22} = \min\left\{\alpha_{22}v_2^{in}\rho_2^{in}, \alpha_{22}\phi_{max,2}^{in}\right\}, \end{aligned}$$

where the first number in the subscript of D is related to the incoming road, and the second number is related to the outgoing road.

In accordance with [25], each outgoing road provides supply for the flow coming from an intersection, which in case of triangular FD (4) reads:

$$\begin{aligned} S_1 &= \min\left\{\omega_1^{out}(\rho_{max,1}^{out} - \rho_1^{out}), \phi_{max,1}^{out}\right\}, \\ S_2 &= \min\left\{\omega_2^{out}(\rho_{max,2}^{out} - \rho_2^{out}), \phi_{max,2}^{out}\right\}. \end{aligned} \tag{6}$$

Let us also *assume* that each outgoing road has a *particular* supply for each incoming road, e.g., S_1 is split into S_{11} and S_{21} (recall that the first number

is referred to an incoming road). In order to define these *partial supplies*, we introduce **supply ratios (SR)** $\beta_{ij} \in [0,1]$ used to denote the proportion of supply of an outgoing road j that it provides for the maximal flow coming from a particular incoming road i relative to the overall supply it provides for all incoming roads. The supply ratio β_{ij} is thus defined as

$$\beta_{ij} = \frac{\alpha_{ij}\phi^{in}_{max,i}}{\sum_{k=1}^{n_{in}} \alpha_{kj}\phi^{in}_{max,k}}, \tag{7}$$

where n_{in} is the number of incoming roads, in this case (Fig. 2) $n_{in} = 2$. Notice that for each outgoing road the sum of its SR must be 1, i.e.,

$$\beta_{11} + \beta_{21} = 1, \quad \beta_{12} + \beta_{22} = 1.$$

With the definition of supply ratios (7), we are now ready to formulate **partial supplies** as the overall (intersection-related) supply given by (6) multiplied by the corresponding SR:

$$S_{ij} = \beta_{ij} S_j = \min\left\{\beta_{ij}\omega^{out}_j(\rho^{out}_{max,j} - \rho^{out}_j), \beta_{ij}\phi^{out}_{max,j}\right\}.$$

Under the assumption of SR, we can also define **partial flows** as the minimum between partial demand and partial supply, i.e., $\phi_{11} = \min\{D_{11}, S_{11}\}$ yields:

$$\phi_{11} = \min\left\{\alpha_{11}v^{in}_1\rho^{in}_1, \beta_{11}\omega^{out}_1(\rho^{out}_{max,1} - \rho^{out}_1), \alpha_{11}\phi^{in}_{max,1}, \beta_{11}\phi^{out}_{max,1}\right\},$$

Finally, the intersection-related flows from incoming and to outgoing roads are expressed as sums of the corresponding partial flows, i.e.,

$$\phi^{in}_1 = \phi_{11} + \phi_{12}, \quad \phi^{in}_2 = \phi_{21} + \phi_{22},$$
$$\phi^{out}_1 = \phi_{11} + \phi_{21}, \quad \phi^{out}_2 = \phi_{12} + \phi_{22}.$$

Thus, we have established a traffic flow model at one particular intersection from Fig. 2 by explicitly deriving expressions for its inflows and outflows that stay in balance.

3.3. Flows at intersections: generalization

We can generalize the calculations from the previous subsection to any intersection with n_{in} incoming roads with densities ρ_i^{in} and flows ϕ_i^{in} for $i \in \{1, \ldots, n_{in}\}$, and n_{out} outgoing roads with densities ρ_j^{out} and flows ϕ_j^{out} for $j \in \{1, \ldots, n_{out}\}$.

Every incoming road i has its own flow demand D_i to enter its source intersection:

$$D_i = \min\left\{v_i^{in}\rho_i^{in}, \phi_{max,i}^{in}\right\}.$$

Then, we define partial demand from road i to road j as

$$D_{ij} = \alpha_{ij} D_i = \min\left\{\alpha_{ij} v_i^{in}\rho_i^{in}, \alpha_{ij}\phi_{max,i}^{in}\right\}.$$

Supply S_j of the outgoing road j is simply given by

$$S_j = \min\left\{\omega_j^{out}(\rho_{max,j}^{out} - \rho_j^{out}), \phi_{max,j}^{out}\right\},$$

which can be multiplied by the supply ratio β_{ij} to obtain a partial supply of road j for traffic from road i. Partial flow ϕ_{ij} from incoming road i towards outgoing road j is then given by

$$\begin{aligned}\phi_{ij} &= \min\left\{D_{ij}, S_{ij}\right\} = \\ &= \min\left\{\alpha_{ij} v_i^{in}\rho_i^{in},\ \beta_{ij}\omega_j^{out}(\rho_{max,j}^{out} - \rho_j^{out}),\ \alpha_{ij}\phi_{max,i}^{in},\ \beta_{ij}\phi_{max,j}^{out}\right\}.\end{aligned} \tag{8}$$

Finally, the flow from incoming road ϕ_i^{in} is the sum over all the flows exiting this road, and the flow into outgoing road ϕ_j^{out} is the sum over all the flows coming into this road:

$$\phi_i^{in} = \sum_{j=1}^{n_{out}} \phi_{ij}, \qquad \phi_j^{out} = \sum_{i=1}^{n_{in}} \phi_{ij}. \tag{9}$$

For a better overview, we have summarized all the notations introduced in this section in Appendix A.1.

4. NEWS formulation

We seek to develop a model capable of predicting the evolution of multi-directional traffic in a general urban network that may also consist of thousands

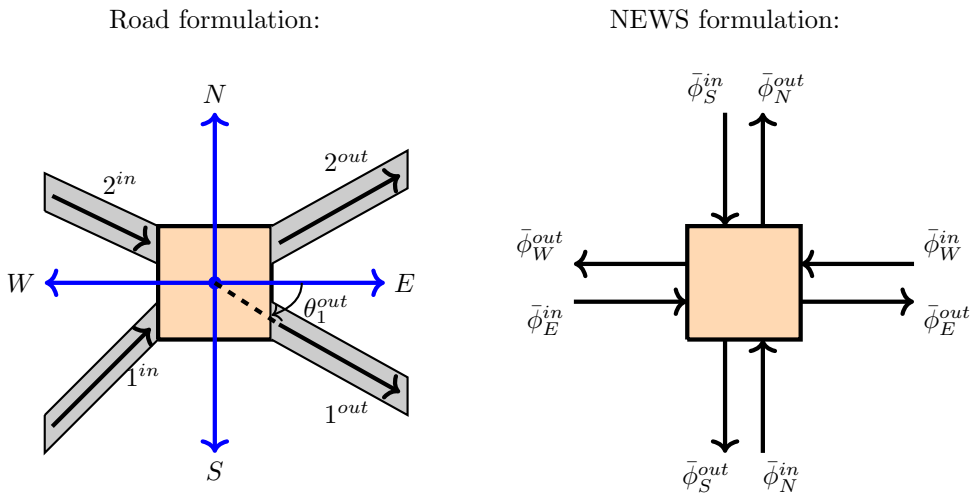

Figure 4: Idea of NEWS framework: map road original directions into North, East, West and South directions, and then traffic flow can be described in terms of 4 direction layers.

of intersections. The main challenge thereby is that roads at every intersection may be oriented arbitrarily. Hence, we would like to obtain a model in terms of flows that are parallel to the cardinal directions: North (**N**), East (**E**), West (**W**) and South (**S**). This will enable us to formulate the model in macroscopic terms, if every intersection will be described in a unified way. Let us call it the **NEWS model**. Its state variables should be denoted by bars, and they represent 4-dimensional vectors, e.g., $\bar{\phi}^{in} = (\bar{\phi}_N^{in}, \bar{\phi}_E^{in}, \bar{\phi}_W^{in}, \bar{\phi}_S^{in})^T$.

Notice that the resulting model is intended to describe the evolution of densities in four direction layers, although an urban area can in general be represented as a 2D plane (x and y). The reason to consider traffic evolution in opposite directions (e.g., North and South) independently is related to the idea to preserve flow values positive, since we want to keep information about the number of vehicles moving in each direction.

4.1. Projection from roads to NEWS

In order to formulate a traffic model in terms of NEWS, *we will use only the geometric properties of the network*, such as angles of road orientations with

respect to the East direction counter-clockwise denoted by θ that ranges from 0 to 2π, see Fig. 4. Thereby, roads 1^{in} and 2^{out} are oriented towards North-East, and roads 2^{in} and 1^{out} are oriented towards South-East.

Let us consider projection of flows into the North. We calculate the flow to the North as a weighted sum of all flows on the roads which have angles less than $\pi/2$ with respect to the North direction, i.e., these are roads 1^{in} and 2^{out} in Fig. 4. This also means that, in general, angle of road's direction with non-zero projection to the North is bounded to the range $\theta \in (0, \pi)$, while for non-zero projections to the South, West and East the angle must be $\theta \in (\pi, 2\pi)$, $\theta \in (\pi/2, 3\pi/2)$ and $\theta \in (0, \frac{\pi}{2}) \cup (\frac{3\pi}{2}, 2\pi)$, respectively. Then, outflows in the NEWS formulation can be found from the road formulation by applying the following projection:

$$\bar{\phi}_N^{out} = p^N_{\theta_1^{out}} \phi_1^{out} + p^N_{\theta_2^{out}} \phi_2^{out}, \qquad \bar{\phi}_E^{out} = p^E_{\theta_1^{out}} \phi_1^{out} + p^E_{\theta_2^{out}} \phi_2^{out},$$
$$\bar{\phi}_W^{out} = p^W_{\theta_1^{out}} \phi_1^{out} + p^W_{\theta_2^{out}} \phi_2^{out}, \qquad \bar{\phi}_S^{out} = p^S_{\theta_1^{out}} \phi_1^{out} + p^S_{\theta_2^{out}} \phi_2^{out},$$

where $p_\theta \in [0, 1]$ are *projection coefficients* that should satisfy the following properties:

1. If a road goes exactly to the North, then $p^N_\theta = 1$.
2. If a road has an angle equal to or greater than $\pi/2$ with the North direction, then $p^N_\theta = 0$.
3. The sum $p^N_\theta + p^E_\theta + p^W_\theta + p^S_\theta = 1$ to ensure the conservation of flows.

Notice that these properties are defined for the North direction, while the same holds also for other directions. The simplest choice for the coefficients p_θ, sat-

isfying all these properties, is

$$
\begin{aligned}
p_\theta^N &= \begin{cases} \dfrac{\sin(\theta)}{|\cos(\theta)| + |\sin(\theta)|}, & \theta \in (0, \pi), \\ 0, & \text{elsewhere}, \end{cases} \\
p_\theta^E &= \begin{cases} \dfrac{\cos(\theta)}{|\cos(\theta)| + |\sin(\theta)|}, & \theta \in (0, \dfrac{\pi}{2}) \cup (\dfrac{3\pi}{2}, 2\pi), \\ 0, & \text{elsewhere}. \end{cases} \\
p_\theta^W &= \begin{cases} \dfrac{-\cos(\theta)}{|\cos(\theta)| + |\sin(\theta)|}, & \theta \in (\dfrac{\pi}{2}, \dfrac{3\pi}{2}), \\ 0, & \text{elsewhere}, \end{cases} \\
p_\theta^S &= \begin{cases} \dfrac{-\sin(\theta)}{|\cos(\theta)| + |\sin(\theta)|}, & \theta \in (\pi, 2\pi), \\ 0, & \text{elsewhere}, \end{cases}
\end{aligned}
\tag{10}
$$

Notice that, in general, *each road can have non-zero weights with at most two directions*. For example, in Fig. 4 flow along the first outgoing road 1^{out} has non-zero weights with South and East direction, i.e., $p^S_{\theta_1^{out}} > 0$ and $p^E_{\theta_1^{out}} > 0$.

4.2. Flows in NEWS formulation

Flows *at each intersection* in NEWS formulation should be given by 4D vectors $\bar{\phi}^{in} = (\bar{\phi}^{in}_N, \bar{\phi}^{in}_E, \bar{\phi}^{in}_W, \bar{\phi}^{in}_S)^T$ and $\bar{\phi}^{out} = (\bar{\phi}^{out}_N, \bar{\phi}^{out}_E, \bar{\phi}^{out}_W, \bar{\phi}^{out}_S)^T$. This allows us to establish the following relation with flows from the original road formulation given by (9) (for the case of Fig. 2):

$$
\bar{\phi}^{in} = \begin{pmatrix} \bar{\phi}^{in}_N \\ \bar{\phi}^{in}_E \\ \bar{\phi}^{in}_W \\ \bar{\phi}^{in}_S \end{pmatrix} = \begin{bmatrix} p^N_{\theta_1^{in}} & p^N_{\theta_2^{in}} \\ p^E_{\theta_1^{in}} & p^E_{\theta_2^{in}} \\ p^W_{\theta_1^{in}} & p^W_{\theta_2^{in}} \\ p^S_{\theta_1^{in}} & p^S_{\theta_2^{in}} \end{bmatrix} \begin{pmatrix} \phi_1^{in} \\ \phi_2^{in} \end{pmatrix}
$$

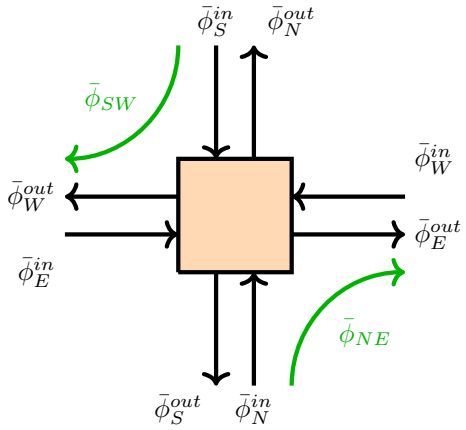

Figure 5: Schemeatic explanation of flow directions in NEWS formulation.

and

$$\bar{\phi}^{out} = \begin{pmatrix} \bar{\phi}_N^{out} \\ \bar{\phi}_E^{out} \\ \bar{\phi}_W^{out} \\ \bar{\phi}_S^{out} \end{pmatrix} = \begin{bmatrix} p^N_{\theta_1^{out}} & p^N_{\theta_2^{out}} \\ p^E_{\theta_1^{out}} & p^E_{\theta_2^{out}} \\ p^W_{\theta_1^{out}} & p^W_{\theta_2^{out}} \\ p^S_{\theta_1^{out}} & p^S_{\theta_2^{out}} \end{bmatrix} \begin{pmatrix} \phi_1^{out} \\ \phi_2^{out} \end{pmatrix}.$$

For a general case of n_{in} incoming and n_{out} outgoing roads, we introduce matrices $P_{in} \in \mathbb{R}^{4\times n_{in}}$ and $P_{out} \in \mathbb{R}^{4\times n_{out}}$ consisting of coefficients $p_{\theta_i^{in}}$ and $p_{\theta_j^{out}}$, respectively. Flows are transformed into the NEWS formulation as follows:

$$\bar{\phi}^{in} = P_{in}\phi^{in}, \quad \bar{\phi}^{out} = P_{out}\phi^{out}. \tag{11}$$

In general, $\bar{\phi}_N^{in}$ is the flow on incoming roads going to the North direction before the intersection, and $\bar{\phi}_N^{out}$ is the flow on outgoing roads going to the North after the intersection, see Fig. 5 for the illustration of this concept. They can also be represented by the sums over *partial flows in the NEWS formulation*:

$$\bar{\phi}_N^{in} = \bar{\phi}_{NN} + \bar{\phi}_{NE} + \bar{\phi}_{NW} + \bar{\phi}_{NS}, \tag{12}$$

and

$$\bar{\phi}_N^{out} = \bar{\phi}_{NN} + \bar{\phi}_{EN} + \bar{\phi}_{WN} + \bar{\phi}_{SN}, \tag{13}$$

where, for example, $\bar{\phi}_{NE}$ is the flow consisting of vehicles going to the North before the intersection and to the East after they have passed the intersection, see Fig. 5. Thus, $\bar{\phi}_N^{in}$ (12) is composed of all such flows that were going to the North before the intersection and then continued their way either to the North or changed to the South, West or East after passing the intersection.

In the NEWS formulation, partial flows are defined from the road formulation as:

$$\bar{\phi}_{EN} = \sum_{i=1}^{n_{in}} \sum_{j=1}^{n_{out}} p^E_{\theta_i^{in}} p^N_{\theta_j^{out}} \phi_{ij}, \tag{14}$$

where p_θ are the projection coefficients from (10). Notice that the correctness of this definition of partial flows can be verified by inserting (14) into (13):

$$\bar{\phi}_N^{out} = \sum_{j=1}^{n_{out}} p^N_{\theta_j^{out}} \left[\sum_{i=1}^{n_{in}} \left(p^N_{\theta_i^{in}} + p^E_{\theta_i^{in}} + p^W_{\theta_i^{in}} + p^S_{\theta_i^{in}} \right) \phi_{ij} \right] =$$
$$\sum_{j=1}^{n_{out}} p^N_{\theta_j^{out}} \sum_{i=1}^{n_{in}} \phi_{ij} = \sum_{j=1}^{n_{out}} p^N_{\theta_j^{out}} \phi_j^{out},$$

whereby we have used the fact that the sum of projection coefficients over all cardinal direction is 1 (see property 3 in the definition of p_θ and (9)).

To gain more insight into the concept of partial flows, let us consider an example of an intersection that has one incoming and one outgoing road, as shown in Fig. 6. First, we define the incoming flow in NEWS formulation from Fig. 6:

$$\bar{\phi}^{in} = \begin{pmatrix} \bar{\phi}_N^{in} \\ \bar{\phi}_E^{in} \\ \bar{\phi}_W^{in} \\ \bar{\phi}_S^{in} \end{pmatrix} = \begin{pmatrix} 0 \\ \bar{\phi}_{EN} + \bar{\phi}_{EE} \\ 0 \\ \bar{\phi}_{SN} + \bar{\phi}_{SE} \end{pmatrix}.$$

Thereby, we see that $\bar{\phi}_N^{in} = \bar{\phi}_W^{in} = 0$, since the incoming road has a zero weight with respect to both North and West direction, while it has non-zero weights with the South and East directions.

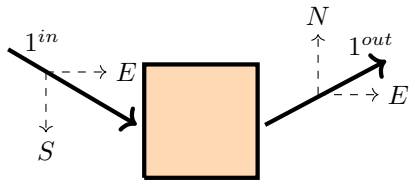

Figure 6: Sketch of an intersection with one incoming road 1^{in} and one outgoing road 1^{out}.

In a similar way, we analyse flow on the outgoing road that yields:

$$\bar{\phi}^{out} = \begin{pmatrix} \bar{\phi}_N^{out} \\ \bar{\phi}_E^{out} \\ \bar{\phi}_W^{out} \\ \bar{\phi}_S^{out} \end{pmatrix} = \begin{pmatrix} \bar{\phi}_{SN} + \bar{\phi}_{EN} \\ \bar{\phi}_{SE} + \bar{\phi}_{EE} \\ 0 \\ 0 \end{pmatrix}.$$

Also note that in Fig. 6 there is no flow in the West direction, therefore all the flows containing at least one "W" are zero, e.g., $\bar{\phi}_{NW} = \bar{\phi}_{SW} = 0$, etc.

4.3. Turning and supply ratios in NEWS formulation

Similar to the traffic model in road formulation given by (9) and (8), we would like to define partial flows in the NEWS formulation using the demand-supply concept (1). For this we will need to define turning $\bar{\alpha}$ and supply ratios $\bar{\beta}$ in the NEWS formulation. Moreover, we will also have to define FD parameters $\bar{v}$, $\bar{\omega}$, $\bar{\rho}_{max}$ in NEWS formulation to be able to derive the complete model.

Demand $\bar{D} \in \mathbb{R}^{4\times 1}$ and supply $\bar{S} \in \mathbb{R}^{4\times 1}$ functions from (4) can be formulated in terms of NEWS using projection coefficient matrices P_{in}, P_{out} as in (11):

$$\begin{aligned} \bar{D} &= P_{in} \min\left\{v^{in}\rho^{in}, \phi_{max}^{in}\right\}, \\ \bar{S} &= P_{out} \min\left\{\omega^{out}(\rho_{max}^{out} - \rho^{out}), \phi_{max}^{out}\right\}. \end{aligned} \tag{15}$$

Now, without loss of generality, let us consider the partial flow from East to North $\bar{\phi}_{EN}$, which we would like to express using demand and supply as in (8):

$$\bar{\phi}_{EN} = \min\left\{\bar{\alpha}_{EN}\bar{D}_E, \bar{\beta}_{EN}\bar{S}_N\right\}, \tag{16}$$

where $\bar{\alpha}_{EN}$ is the turning ratio from East to North, and $\bar{\beta}_{EN}$ is the supply ratio provided by the North for vehicles arriving from the East, i.e., the same as β_{ij} from (7) but in the NEWS formulation.

The coefficients $\bar{\alpha}_{EN}$ and $\bar{\beta}_{EN}$ need to be determined, which can be done using (14), in which we substitute (8) that yields

$$\bar{\phi}_{EN} = \sum_{i=1}^{n_{in}} \sum_{j=1}^{n_{out}} p^{E}_{\theta^{in}_i} p^{N}_{\theta^{out}_j} \min\left\{\alpha_{ij} v_i^{in} \rho_i^{in},\, \beta_{ij} \omega_j^{out} (\rho_{max,j}^{out} - \rho_j^{out}),\, \alpha_{ij} \phi_{max,i}^{in},\, \beta_{ij} \phi_{max,j}^{out}\right\}.$$

This expression is a sum over minimum functions, which is tedious to handle. We make the following *approximation*: change the order of taking the minimum and the summations. This leads to the minimum function over just four arguments as in the demand-supply concept (8):

$$\bar{\phi}_{EN} \approx \min\left\{\sum_{j=1}^{n_{out}} p^{N}_{\theta^{out}_j} \sum_{i=1}^{n_{in}} p^{E}_{\theta^{in}_i} \alpha_{ij} v_i^{in} \rho_i^{in}, \sum_{j=1}^{n_{out}} p^{N}_{\theta^{out}_j} \sum_{i=1}^{n_{in}} p^{E}_{\theta^{in}_i} \beta_{ij} \omega_j^{out} (\rho_{max,j}^{out} - \rho_j^{out}), \dots\right\}.$$

Notice that the difference between putting minimum inside and outside the summation is decreasing as the level of the homogeneity in the congestion of links increases. This approximation is exact if all roads in the network are in the same traffic regime, i.e., either all roads are in free-flow or congested.

We set the latter expression equal to (16) for $\phi = \phi_{max}$, and get the coefficients $\bar{\alpha}_{EN}$ and $\bar{\beta}_{EN}$ that read

$$\bar{\alpha}_{EN} = \frac{\sum\limits_{j=1}^{n_{out}} \left[p^{N}_{\theta^{out}_j} \sum\limits_{i=1}^{n_{in}} \alpha_{ij} p^{E}_{\theta^{in}_i} \phi_{max,i}^{in} \right]}{\sum\limits_{i=1}^{n_{in}} p^{E}_{\theta^{in}_i} \phi_{max,i}^{in}}, \tag{17}$$

and

$$\bar{\beta}_{EN} = \frac{\sum\limits_{i=1}^{n_{in}} \left[p^{E}_{\theta^{in}_i} \sum\limits_{j=1}^{n_{out}} \beta_{ij} p^{N}_{\theta^{out}_j} \phi_{max,j}^{out} \right]}{\sum\limits_{j=1}^{n_{out}} p^{N}_{\theta^{out}_j} \phi_{max,j}^{out}}. \tag{18}$$

4.4. FD parameters and densities in NEWS formulation

Consider demand and supply functions in the NEWS formulation. From one side, we can calculate them using the projection matrices P_{in} and P_{out} as in (15). From the other side, we would like to be able to calculate demand and

supply using fundamental diagram, which should enable us to describe traffic flow in a unified way for any intersection. Recall that FD parameters are space-dependent, i.e., they depend on a specific road, since different roads might have different speed limits or capacity.

Hence, we are going to define a unified FD in NEWS formulation such that the FD is defined for each direction separately. This equivalently means that the parameters of FD will all become 4-dimensional vectors or 4×4 diagonal matrices. Let us consider the FD for the North direction, while similar steps should be done for other directions. That is, for $\bar{D}_N$ and $\bar{S}_N$ we would like to find kinematic wave speeds $\bar{v}_N^{in}$ and $\bar{\omega}_N^{out}$ and density transformations $\bar{\rho}_N^{in}$ and $\bar{\rho}_N^{out}$ such that the following relations would hold:

$$\bar{D}_N = \sum_{i=1}^{n_{in}} p_i^N \min\{v_i\rho_i, \phi_{max,i}\} \approx \min\left\{\bar{v}_N^{in}\bar{\rho}_N^{in}, \bar{\phi}_{max,N}^{in}\right\},$$
$$\bar{S}_N = \sum_{j=1}^{n_{out}} p_j^N \min\{\omega_j(\rho_{max,j} - \rho_j), \phi_{max,j}\} \approx \min\left\{\bar{\omega}_N^{out}(\bar{\rho}_{max,N} - \bar{\rho}_N^{out}), \bar{\phi}_{max,N}^{out}\right\}.$$

Note that in the case when an intersection has much more than 4 roads, we can use only approximations of the fundamental diagram.

By approximating sum of minimum functions as a minimum of sums and writing the conditions on maximal flows together, we get the system

$$\begin{aligned} \sum_{i=1}^{n_{in}} p_i^N v_i \rho_{c,i} &= \bar{v}_N^{in}\bar{\rho}_{c,N}^{in}, \\ \sum_{j=1}^{n_{out}} p_j^N \omega_j(\rho_{max,j} - \rho_{c,j}) &= \bar{\omega}_N^{out}(\bar{\rho}_{max,N}^{out} - \bar{\rho}_{c,N}^{out}). \end{aligned} \tag{19}$$

System (19) is undetermined since it consists of two equations that have five unknowns $(\bar{v}_N^{in}, \bar{\omega}_N^{out}, \bar{\rho}_{c,N}^{in}, \bar{\rho}_{c,N}^{out}, \bar{\rho}_{max,N}^{out})$.

In general, we get the coordinates of each road, its number of lanes and speed limits as network data. Speed limits are directly related to the kinematic wave speeds v_j, while the maximal density $\rho_{max,j}$ on each road j (either incoming or outgoing) is determined by its number of lanes and the minimal car-to-car distance (we assume it to be 6 m). Knowing $\rho_{max,j}$ for every road, we can easily

obtain the critical density $\rho_{c,j}$ from the shape of the fundamental diagram (that is commonly an experimentally established function). Negative kinematic wave speeds ω_j can be obtained from the speed limits v_j and critical density $\rho_{c,j}$ as

$$\omega_j = \frac{\rho_{c,j} v_j}{\rho_{max,j} - \rho_{c,j}}.$$

Both incoming and outgoing roads contribute to the vehicle density in some intersection's neighbourhood. Moreover, since we want to have a general model, which is symmetric with respect to incoming and outgoing roads, and in order to define each parameter only once, we assume symmetry $\bar{\rho}_N^{in} = \bar{\rho}_N^{out} = \bar{\rho}_N$, $\bar{v}_N^{in} = \bar{v}_N^{out} = \bar{v}_N$ and $\bar{\omega}_N^{in} = \bar{\omega}_N^{out} = \bar{\omega}_N$.

Assume further that densities are transformed into NEWS formulation in the same way as it is done for the flows (11), i.e.:

$$\bar{\rho}_N = \sum_{i=1}^{n_{in}} p_i^N \rho_i + \sum_{j=1}^{n_{out}} p_j^N \rho_j, \tag{20}$$

which then also holds for maximal $\bar{\rho}_{max,N}$ and critical $\bar{\rho}_{c,N}$ densities. After we have defined all the densities, using symmetry assumption we can express the velocities from (19) as

$$\bar{v}_N = \frac{\sum_{i=1}^{n_{in}} p_i^N v_i \rho_{c,i} + \sum_{j=1}^{n_{out}} p_j^N v_j \rho_{c,j}}{\bar{\rho}_{c,N}},$$

$$\bar{\omega}_N = \frac{\sum_{i=1}^{n_{in}} p_i^N \omega_i (\rho_{max,i} - \rho_{c,i}) + \sum_{j=1}^{n_{out}} p_j^N \omega_j (\rho_{max,j} - \rho_{c,j})}{\bar{\rho}_{max,N} - \bar{\rho}_{c,N}}.$$

Recall that all these calculations are not limited to the particular triangular shape of FD, and thus can be performed in the same way for any type of FD as long as it is a concave function of density as it is also assumed in the LWR model (see Remark 1). The only thing that would have changed for different FD shapes are formulas for its parameters (19), since each FD can have a different set of parameters.

For a better overview, we have summarized all the NEWS-related notations introduced in this and next sections in Appendix A.2.

5. Derivation of the NEWS model

Our main goal is to derive the macroscopic NEWS model for multi-directional traffic that can describe the dynamic evolution of traffic state similar to LWR model as stated in Section 2. For the moment, we can already describe traffic flow for any intersection in the unified way, which became possible due to the concept of partial flows in the NEWS formulation given by (16) with (17) and (18). The dynamic NEWS model in terms of density will be derived by considering an intersection and its outgoing roads that should be viewed as incoming roads for the neighbouring intersections. In the end, we will be able to describe the whole urban area due to a unified description of the traffic behaviour at any intersection. This unified description will be obtained using the continuation method that has just been introduced in [43].

5.1. Continuation

Previously, we considered inflows ϕ^{in} and outflows ϕ^{out} with respect to some intersection. However, for the derivation of the macroscopic continuum model, we consider inflows and outflows with respect to roads that will be denoted by ψ^{in} and ψ^{out} as in Fig. 7.

Recall that θ is an angle between the road orientation and the East direction. Denote the flow in the direction θ as ψ_θ. Essentially, there are two flows with direction θ: inflow ψ_θ^{in} which is a sum of all flows incoming in a road with orientation θ, and outflow ψ_θ^{out} which is a sum of all flows outgoing from this road. Notice that, in the following, we will deal *only with outgoing roads*. Thus, we skip the superscript in the notation of angle, i.e., $\theta_j^{out} = \theta_j$.

Now consider some road j of length l_j that is an outgoing road for the intersection located at (x_1, y_1), see Fig. 7. The density evolution on road j that is connecting the intersection at (x_1, y_1) and the intersection at (x_2, y_2) is

$$\frac{\partial \rho_j}{\partial t} = \frac{1}{l_j}\left(\psi_{\theta_j}^{in}(x_1, y_1) - \psi_{\theta_j}^{out}(x_2, y_2)\right),$$

where $\theta_j = \mathrm{atan}[(y_2 - y_1)/(x_2 - x_1)]$ as in Fig. 7. Notice that there are no bars here in the notations, since we again refer to the road formulation.

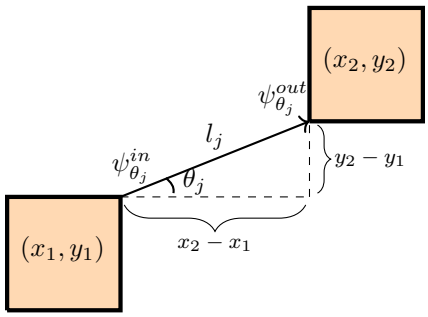

Figure 7: Illustration of notations used for derivation of the NEWS model.

The equation written above depends on two different space points (x_1, y_1) and (x_2, y_2). However, we would like to obtain an equation that is given for a unique point of space. In order to achieve that, we can perform continuation at the beginning of the road (x_1, y_1). In its simplest form, the continuation method corresponds to the first-order term of Taylor expansion in spatial coordinates, which reads:

$$\psi^{out}_{\theta_j}(x_2, y_2) \approx \psi^{out}_{\theta_j}(x_1, y_1) + (x_2 - x_1)\frac{\partial \psi^{out}_{\theta_j}}{\partial x} + (y_2 - y_1)\frac{\partial \psi^{out}_{\theta_j}}{\partial y},$$

and assuming this approximation to be an equality, we get the following model

$$\frac{\partial \rho_j}{\partial t} = \frac{1}{l_j}\left(\psi^{in}_{\theta_j}(x_1, y_1) - \psi^{out}_{\theta_j}(x_1, y_1) - (x_2 - x_1)\frac{\partial \psi^{out}_{\theta_j}}{\partial x} - (y_2 - y_1)\frac{\partial \psi^{out}_{\theta_j}}{\partial y}\right),$$

or simply

$$\frac{\partial \rho_j}{\partial t} = \frac{1}{l_j}\left(\psi^{in}_{\theta_j}(x_1, y_1) - \psi^{out}_{\theta_j}(x_1, y_1)\right) - \cos\theta_j \frac{\partial \psi^{out}_{\theta_j}}{\partial x} - \sin\theta_j \frac{\partial \psi^{out}_{\theta_j}}{\partial y}.$$

At the same time, by performing continuation at the end of the road (x_2, y_2) we arrive at

$$\frac{\partial \rho_j}{\partial t} = \frac{1}{l_j}\left(\psi^{in}_{\theta_j}(x_2, y_2) - \psi^{out}_{\theta_j}(x_2, y_2)\right) - \cos\theta_j \frac{\partial \psi^{in}_{\theta_j}}{\partial x} - \sin\theta_j \frac{\partial \psi^{in}_{\theta_j}}{\partial y}.$$

Since the density along the road is assumed to be constant, both continuous models can be used to represent the original one. The first model is defined in terms of the beginning of the road (x_1, y_1) and contains spatial derivatives of

$\psi^{out}_{\theta_j}$, whereas the second model is defined in terms of the end of the road (x_2, y_2) and contains spatial derivatives of $\psi^{in}_{\theta_j}$. However, performing continuation not at the end points but somewhere in between can result into a more general form that unifies these two models.

Let us perform continuation of the model for some arbitrary point along the road (x, y) whose coordinates lie between two endpoints (x_1, y_1) and (x_2, y_2):

$$x = x_1\gamma + x_2(1-\gamma), \qquad y = y_1\gamma + y_2(1-\gamma),$$

where $\gamma \in [0, 1]$. Thus, by performing continuation at (x, y), we arrive at

$$\begin{aligned}\frac{\partial \rho_j}{\partial t} = \frac{1}{l_j}\left(\psi^{in}_{\theta_j}(x,y) - \psi^{out}_{\theta_j}(x,y)\right) - \cos\theta_j \frac{\partial((1-\gamma)\psi^{in}_{\theta_j} + \gamma\psi^{out}_{\theta_j})}{\partial x} \\ - \sin\theta_j \frac{\partial((1-\gamma)\psi^{in}_{\theta_j} + \gamma\psi^{out}_{\theta_j})}{\partial y}.\end{aligned} \tag{21}$$

Now let the vector-flow on road j be

$$\vec{\Psi}_{\theta_j} = \psi_{\theta_j}\begin{pmatrix}\cos\theta_j \\ \sin\theta_j\end{pmatrix}, \quad \text{where} \quad \psi_{\theta_j} = (1-\gamma)\psi^{in}_{\theta_j} + \gamma\psi^{out}_{\theta_j}.$$

Then, the model (21) can be rewritten as

$$\frac{\partial \rho_j}{\partial t} = \frac{1}{l_j}\left(\psi^{in}_{\theta_j}(x,y) - \psi^{out}_{\theta_j}(x,y)\right) - \nabla \cdot \vec{\Psi}_{\theta_j}(x,y), \tag{22}$$

where ∇ is a nabla operator defined as $\nabla = (\frac{\partial}{\partial x}, \frac{\partial}{\partial y})$.

This model (22) predicts the dynamics of vehicle density at some outgoing road j with direction θ_j. Equation (22) has the same form for any intersection located at (x_k, y_k), where $k \in \{1, \ldots, K\}$ is an index used to label intersections in the domain of interest. Notice that parameter γ was introduced only for the derivation purposes, it will not explicitly appear in the final model, see details below.

5.2. The NEWS model

We would like to translate the model given in road formulation (22) into NEWS formulation. Recall that densities in every direction layer are transformed as in (20). Let us again consider the North direction for simplicity, while the same steps should be performed for all other directions.

Thus, multiplying the equation (22) by $p^N_{\theta_j}$ and taking the summation, we get the model that predicts the evolution of vehicle density in the North direction on outgoing roads of an intersection located at (x_k, y_k) that reads

$$\frac{\partial \bar{\rho}_N}{\partial t} = \sum_{j=1}^{n_{out}} p^N_{\theta_j} \frac{1}{l_j} \left(\psi^{in}_{\theta_j} - \psi^{out}_{\theta_j} \right) - \nabla \cdot \left(\sum_{j=1}^{n_{out}} p^N_{\theta_j} \vec{\Psi}_{\theta_j} \right). \tag{23}$$

We cannot further simplify the equation (23) towards the NEWS formulation, since the summations contain additional index-dependent coefficients such as $1/l_j$, $\sin\theta_j$ and $\cos\theta_j$ (embedded in $\vec{\Psi}_{\theta_j}$). Let us then approximate the system (23) by averaging road lengths l_j such that the mean length of outgoing roads conserves the maximum number of cars:

$$L = \frac{\sum\limits_{j=1}^{n_{out}} \rho_{max,j} l_j}{\sum\limits_{j=1}^{n_{out}} \rho_{max,j}}.$$

Further, we also approximate sine and cosine in (23) as

$$\overline{\cos\theta}_N = \frac{\sum\limits_{j=1}^{n_{out}} p^N_{\theta_j} \cos\theta_j \phi_{max,j}}{\sum\limits_{j=1}^{n_{out}} p^N_{\theta_j} \phi_{max,j}}, \qquad \overline{\sin\theta}_N = \frac{\sum\limits_{j=1}^{n_{out}} p^N_{\theta_j} \sin\theta_j \phi_{max,j}}{\sum\limits_{j=1}^{n_{out}} p^N_{\theta_j} \phi_{max,j}}.$$

Substituting these approximations into (23), we get

$$\begin{aligned} \frac{\partial \bar{\rho}_N}{\partial t} = {} & \frac{1}{L} \sum_{j=1}^{n_{out}} p^N_{\theta_j} \left(\psi^{in}_{\theta_j} - \psi^{out}_{\theta_j} \right) \\ & - \nabla \cdot \left(\sum_{j=1}^{n_{out}} \begin{pmatrix} \overline{\cos\theta}_N \\ \overline{\sin\theta}_N \end{pmatrix} p^N_{\theta_j} \left((1-\gamma)\psi^{in}_{\theta_j} + \gamma \psi^{out}_{\theta_j} \right) \right), \end{aligned}$$

or simply

$$\frac{\partial \bar{\rho}_N}{\partial t} = \frac{1}{L} \left(\bar{\psi}^{in}_N - \psi^{out}_N \right) - \nabla \cdot \left(\begin{pmatrix} \overline{\cos\theta}_N \\ \overline{\sin\theta}_N \end{pmatrix} \left((1-\gamma)\bar{\psi}^{in}_N + \gamma \bar{\psi}^{out}_N \right\langle \right) \right), \tag{24}$$

where we can further define $\bar{\psi}_N = (1-\gamma)\bar{\psi}^{in}_N + \gamma \bar{\psi}^{out}_N$.

Notice that (24) is already very close to the macroscopic NEWS model (see Sec. 2), since it does not depend on road index j any more. In some sense,

the model (24) is defined for any particular space point in the vicinity of an intersection. Therefore, it makes no more sense to have separate notations for flows related to intersections $\bar{\phi}$ and roads $\bar{\psi}$. For convenience and consistency with other parts of this paper, we will again use the notation $\bar{\phi}$ for flows.

The model (24) can be further simplified in order to get rid of spatial derivatives over multi-directional flows, since otherwise the PDE can lose hyperbolicity and, moreover, we want to eliminate the parameter γ.

5.3. Model simplification

The term under the space derivative in (24) is $\bar{\phi}_N = (1-\gamma)\bar{\phi}_N^{in} + \gamma\bar{\phi}_N^{out}$. Recall that by (12) and (13) we can express inflows and outflows at any point as sums over partial flows:

$$\begin{aligned}\bar{\phi}_N^{in} &= \bar{\phi}_{NN} + \bar{\phi}_{EN} + \bar{\phi}_{WN} + \bar{\phi}_{SN},\\ \bar{\phi}_N^{out} &= \bar{\phi}_{NN} + \bar{\phi}_{NE} + \bar{\phi}_{NW} + \bar{\phi}_{NS}.\end{aligned}$$

Therefore, we can insert this definition into $\bar{\phi}_N$ and get

$$\begin{aligned}\bar{\phi}_N = \bar{\phi}_{NN} &+ \left[(1-\gamma)\bar{\phi}_{EN} + \gamma\bar{\phi}_{NE}\right] +\\ &+ \left[(1-\gamma)\bar{\phi}_{WN} + \gamma\bar{\phi}_{NW}\right] + \left[(1-\gamma)\bar{\phi}_{SN} + \gamma\bar{\phi}_{NS}\right].\end{aligned} \tag{25}$$

This means that (24) requires taking spatial derivatives over multi-directional flows. However, the model (24) would be considerably simplified if each term under the spatial derivative could be written only as a function of demand and supply of the corresponding direction, i.e.,

$$\bar{\phi}_N = \min\{\bar{D}_N, \bar{S}_N\}. \tag{26}$$

Now we make an assumption that *the network is well-designed in terms of maximal flows*, that is

$$\bar{\alpha}_{NE}\bar{\phi}_{max,N} = \bar{\beta}_{NE}\bar{\phi}_{max,E}. \tag{27}$$

Physically, this assumption means that if vehicles move at maximal possible flow before an intersection, they continue to use roads' transportation capacities at maximum after the intersection.

The proof that (26) holds under the assumption of a well-designed network (27), being rather technical, is shifted to Appendix Appendix B, where we show that there exists parameter γ such that (26) holds. Thus, the transported term under the derivative in (24) can be approximated by a standard flow in the demand-supply formulation that depends only on the density of the same direction. Hence, the full system of equations can be written as

$$\begin{cases} \dfrac{\partial \bar{\rho}_N}{\partial t} = \dfrac{1}{L}\left(\bar{\phi}_N^{in} - \bar{\phi}_N^{out}\right) - \dfrac{\partial(\overline{\cos\theta}_N \bar{\phi}_N)}{\partial x} - \dfrac{\partial(\overline{\sin\theta}_N \bar{\phi}_N)}{\partial y}, \\ \dfrac{\partial \bar{\rho}_E}{\partial t} = \dfrac{1}{L}\left(\bar{\phi}_E^{in} - \bar{\phi}_E^{out}\right) - \dfrac{\partial(\overline{\cos\theta}_E \bar{\phi}_E)}{\partial x} - \dfrac{\partial(\overline{\sin\theta}_E \bar{\phi}_E)}{\partial y}, \\ \dfrac{\partial \bar{\rho}_W}{\partial t} = \dfrac{1}{L}\left(\bar{\phi}_W^{in} - \bar{\phi}_W^{out}\right) - \dfrac{\partial(\overline{\cos\theta}_W \bar{\phi}_W)}{\partial x} - \dfrac{\partial(\overline{\sin\theta}_W \bar{\phi}_W)}{\partial y}, \\ \dfrac{\partial \bar{\rho}_S}{\partial t} = \dfrac{1}{L}\left(\bar{\phi}_S^{in} - \bar{\phi}_S^{out}\right) - \dfrac{\partial(\overline{\cos\theta}_S \bar{\phi}_S)}{\partial x} - \dfrac{\partial(\overline{\sin\theta}_S \bar{\phi}_S)}{\partial y}, \end{cases} \tag{28}$$

where the term $\bar{\phi}^{in} - \bar{\phi}^{out}$ is given by

$$\begin{pmatrix} \bar{\phi}_N^{in} - \bar{\phi}_N^{out} \\ \bar{\phi}_E^{in} - \bar{\phi}_E^{out} \\ \bar{\phi}_W^{in} - \bar{\phi}_W^{out} \\ \bar{\phi}_S^{in} - \bar{\phi}_S^{out} \end{pmatrix} = \begin{pmatrix} \bar{\phi}_{EN} + \bar{\phi}_{WN} + \bar{\phi}_{SN} - \bar{\phi}_{NE} - \bar{\phi}_{NW} - \bar{\phi}_{NS} \\ \bar{\phi}_{NE} + \bar{\phi}_{WE} + \bar{\phi}_{SE} - \bar{\phi}_{EN} - \bar{\phi}_{EW} - \bar{\phi}_{ES} \\ \bar{\phi}_{NW} + \bar{\phi}_{EW} + \bar{\phi}_{SW} - \bar{\phi}_{WN} - \bar{\phi}_{WE} - \bar{\phi}_{WS} \\ \bar{\phi}_{NS} + \bar{\phi}_{ES} + \bar{\phi}_{WS} - \bar{\phi}_{SN} - \bar{\phi}_{SE} - \bar{\phi}_{SW} \end{pmatrix}.$$

This system of equations describes the density evolution in the vicinity of one intersection, and it coincides with the goal stated in Sec. 2. Thus, the density $\bar{\rho}(x, y, t)$ and the flow $\bar{\phi}(x, y, t)$ are space- and time-dependent functions, whereas all the parameters are still constant ($\bar{\alpha}$, $\bar{\beta}$, L, $\bar{v}$, $\bar{\omega}$, $\bar{\rho}_{max}$, $\overline{\cos\theta}$, $\overline{\sin\theta}$).

Notice that the term $\bar{\phi}^{in} - \bar{\phi}^{out}$ is responsible for mixing between different density layers, e.g., $\bar{\phi}_N^{in} = \bar{\phi}_{SN} + \bar{\phi}_{WN} + \bar{\phi}_{EN}$ accounts for vehicles that were moving to the South, West and East, and then turned to the North.

System (28) together with a 4-dimensional fundamental diagram that can be any concave Lipschitz continuous vector function) represents the **NEWS model**, which is one of the main results of this paper. It models the evolution of vehicle density on outgoing roads of an intersection in all cardinal directions: North, East, West and South.

The last step that needs to be taken is to obtain a continuous PDE system describing traffic flow propagation in the *whole network*. This can be done by

approximating the entire parameters of system (28) over the whole continuum domain. First, we calculate $\bar{\alpha}$, $\bar{\beta}$, L, $\bar{v}$, $\bar{\omega}$, $\bar{\rho}_{max}$, $\overline{\cos\theta}$, $\overline{\sin\theta}$ for all K intersections in the network. Then, we are looking for functions that approximate all these parameters over a continuum plane, e.g., the value of an average road length can be defined $\forall(x, y) \in R^2$

$$L(x,y) = \frac{\sum_{k=1}^{K} L(x_k, y_k) e^{-\eta\sqrt{(x-x_k)^2+(y-y_k)^2}}}{\sum_{k=1}^{K} e^{-\eta\sqrt{(x-x_k)^2+(y-y_k)^2}}}, \tag{29}$$

where η is a weighting parameter used to denote the sensitivity of the estimated variables to the distance from the intersections. This approximation method is called Inverse Distance Weighting, where we chose an exponential function to give larger weights to close intersections, see also [38].

Thus, we define all the geometrical and FD parameters $\forall(x, y)$, and obtain a continuous PDE system that looks like (28) with time- and space-dependent density $\bar{\rho}(x, y, t)$ and flow $\bar{\phi}(x, y, \bar{\rho})$, while all parameters become **space-dependent** (but time- and state-independent) functions due to (29), i.e., $\bar{\alpha}(x, y)$, $\bar{\beta}(x, y)$, $\bar{v}(x, y)$, etc. As a result we obtain the NEWS model as stated in Sec. 2. See also Fig. 1 for the summary of all the steps required for the model derivation.

Remark 2. The obtained model has a structure of a PDE system, and its main advantage is its simplicity of formulation. That is, it describes traffic state in the whole area under consideration using only four equations, i.e., it has a convenient form for explicit analysis and control design. Being used as a prediction tool in a simulation, the model should be discretized, and thus a trade-off between computational time and the number of cells appears. As a general rule of thumb, one should take cells small enough such that the density profile inside can be assumed homogeneous (as in LWR).

5.4. Extended model with source and sink terms

In an urban network of finite size there exist roads, through which cars can enter or exit the domain. Such roads are called sources and sinks, respectively.

The upstream and downstream boundary conditions for the PDE system (28) are directly determined by these sources and sinks, respectively. It appears that they can be trivially captured by the NEWS model. Let us now show how sources are implemented into the model (28), while the implementation of sinks can be done in the same way.

We consider some road j through which exterior vehicles enter at flow $\psi_{\theta_j}^{source}$ (we use again ψ for flow, since it is here formulated in terms of roads). We take this additional flow of vehicles into account by adding it into equation (22) for road j, which yields

$$\frac{\partial \rho_j}{\partial t} = \frac{1}{l_j}\left(\psi_{\theta_j}^{in} - \psi_{\theta_j}^{out}\right) - \nabla \cdot \vec{\Psi}_{\theta_j} + \frac{1}{l_j}\psi_{\theta_j}^{source}. \tag{30}$$

In general, we have to deal with the demand-supply problem also in order to specify inflow for some road, i.e., we can only propose it as a demand function. Then, the amount of flow entering this road depends also on its supply, which is in turn determined by the state:

$$\psi_{\theta_j}^{source} = \min\left\{D_{\theta_j}^{source}, S_{\theta_j}(\rho_j)\right\}.$$

We can rewrite (30) in NEWS formulation by performing the transformations described in Sec. 5.2, which leads us to the extended NEWS model (with sinks also included):

$$\begin{cases} \dfrac{\partial \bar{\rho}_N}{\partial t} = \dfrac{1}{L}\left(\bar{\phi}_N^{in} - \bar{\phi}_N^{out} + \bar{\phi}_N^{source} - \bar{\phi}_N^{sink}\right) - \dfrac{\partial(\overline{\cos\theta}_N \bar{\phi}_N)}{\partial x} - \dfrac{\partial(\overline{\sin\theta}_N \bar{\phi}_N)}{\partial y}, \\ \dfrac{\partial \bar{\rho}_E}{\partial t} = \dfrac{1}{L}\left(\bar{\phi}_E^{in} - \bar{\phi}_E^{out} + \bar{\phi}_E^{source} - \bar{\phi}_E^{sink}\right) - \dfrac{\partial(\overline{\cos\theta}_E \bar{\phi}_E)}{\partial x} - \dfrac{\partial(\overline{\sin\theta}_E \bar{\phi}_E)}{\partial y}, \\ \dfrac{\partial \bar{\rho}_W}{\partial t} = \dfrac{1}{L}\left(\bar{\phi}_W^{in} - \bar{\phi}_W^{out} + \bar{\phi}_W^{source} - \bar{\phi}_W^{sink}\right) - \dfrac{\partial(\overline{\cos\theta}_W \bar{\phi}_W)}{\partial x} - \dfrac{\partial(\overline{\sin\theta}_W \bar{\phi}_W)}{\partial y}, \\ \dfrac{\partial \bar{\rho}_S}{\partial t} = \dfrac{1}{L}\left(\bar{\phi}_S^{in} - \bar{\phi}_S^{out} + \bar{\phi}_S^{source} - \bar{\phi}_S^{sink}\right) - \dfrac{\partial(\overline{\cos\theta}_S \bar{\phi}_S)}{\partial x} - \dfrac{\partial(\overline{\sin\theta}_S \bar{\phi}_S)}{\partial y}, \end{cases} \tag{31}$$

where, e.g., $\bar{\phi}_N^{source}(x,y,t)$ and $\bar{\phi}_N^{sink}(x,y,t)$ are space- and time dependent boundary flows given by a demand-supply problem

$$\bar{\phi}_N^{source} = \min\{\bar{D}_N^{source}, \bar{S}_N\}, \qquad \bar{\phi}_N^{sink} = \min\{\bar{D}_N, \bar{S}_N^{sink}\},$$

with

$$\bar{D}_N^{source} = \sum_{j=1}^{n_{out}} p_{\theta_j}^N D_{\theta_j}^{source}, \qquad \bar{S}_N^{sink} = \sum_{j=1}^{n_{out}} p_{\theta_j}^N S_{\theta_j}^{sink}.$$

Further, one needs to approximate $\bar{D}_N^{source}$ and $\bar{S}_N^{sink}$ in the whole domain, since originally we specify it in terms of roads of the network. In contrast to all other variables obtained by (29), the overall number of incoming cars should be conserved. Thus, we choose Gaussian kernel for the approximation of demand and supply functions:

$$\bar{D}_N^{source}(x,y) = \sum_{k=1}^{K} \bar{D}_N^{source}(x_k,y_k) G_\sigma(x-x_k, y-y_k),$$

where $G_\sigma(x,y)$ is a two-dimensional symmetric Gaussian kernel with σ being its standard deviation:

$$G_\sigma(x,y) = \frac{1}{2\pi\sigma^2} e^{-\frac{1}{2\sigma^2}\left(x^2+y^2\right)}.$$

Parameter σ can be tuned to change the radius of influence of demand and supply functions around the intersection. Note that such a choice of $G_\sigma(x,y)$ provides that its integral over the whole domain equals 1, therefore the overall incoming demand in (31) is the same as in the original network model (30) (road formulation).

6. Mathematical properties of NEWS model

Let us now investigate the properties of the NEWS model. For its explicit analysis, we take system (28) that does not include any source terms. In this section we will check whether our system represents a conservation law, then we will discuss the boundedness of its state $\bar{\rho}$, and, finally, we will show that NEWS model represents a hyperbolic PDE system.

6.1. Conservation law

The overall density in the network is the sum over densities in all four direction layers, that is

$$\bar{\rho} = \bar{\rho}_N + \bar{\rho}_E + \bar{\rho}_W + \bar{\rho}_S.$$

By taking its time derivative we get

$$\frac{\partial \bar{\rho}}{\partial t} = \frac{\partial \bar{\rho}_N}{\partial t} + \frac{\partial \bar{\rho}_E}{\partial t} + \frac{\partial \bar{\rho}_W}{\partial t} + \frac{\partial \bar{\rho}_S}{\partial t},$$

and for each of these terms we can substitute the corresponding PDE from our model (28). It appears that all the mixing terms ($\bar{\phi}^{in} - \bar{\phi}^{out}$) cancel each other, and we simply get:

$$\frac{\partial \bar{\rho}}{\partial t} = -\nabla \cdot \bar{\Phi}, \tag{32}$$

where

$$\bar{\Phi} = \begin{pmatrix} \overline{\cos\theta}_N \\ \overline{\sin\theta}_N \end{pmatrix} \bar{\phi}_N + \begin{pmatrix} \overline{\cos\theta}_E \\ \overline{\sin\theta}_E \end{pmatrix} \bar{\phi}_E + \begin{pmatrix} \overline{\cos\theta}_W \\ \overline{\sin\theta}_W \end{pmatrix} \bar{\phi}_W + \begin{pmatrix} \overline{\cos\theta}_S \\ \overline{\sin\theta}_S \end{pmatrix} \bar{\phi}_S,$$

which has a form of a conservation law, where the conserved quantity is the overall density in the network.

6.2. Boundedness of the state

The boundedness of the density $\bar{\rho} \in [0, \bar{\rho}_{max}]$ is not violated in our model (28), since the terms under the derivatives are resolved using the standard Godunov scheme, i.e., traffic flow in each direction is determined by the minimum between demand and supply, as in LWR formalism. For example, consider the North direction, then the term under the spatial derivative in (28) is just

$$\bar{\phi}_N = \min\left\{\bar{D}_N, \bar{S}_N\right\}.$$

Mixing terms with a positive sign (these are $\bar{\phi}_{EN}$, $\bar{\phi}_{WN}$ and $\bar{\phi}_{SN}$ in the equation for $\bar{\rho}_N$) depend on the supply of N, e.g.,

$$\bar{\phi}_{EN} = \min\left\{\bar{\alpha}_{EN}\bar{D}_E, \bar{\beta}_{EN}\bar{S}_N\right\}.$$

If $\bar{\rho}_N = \bar{\rho}_{max,N}$, then

$$\bar{S}_N = 0 \Rightarrow \bar{\phi}_{EN} = 0 \Rightarrow \frac{\partial \bar{\rho}_N}{\partial t} \leq 0,$$

which means that positive terms can not contribute to the increase of density when it has reached $\bar{\rho}_{max,N}$.

Let us now consider negative mixing terms. These depend on the demand of the North direction layer, e.g.,

$$\bar{\phi}_{NE} = \min\left\{\bar{\alpha}_{NE}\bar{D}_N, \bar{\beta}_{NE}\bar{S}_E\right\},$$

which in case of $\bar{\rho}_N = 0 \Rightarrow D_N = 0$ yields:

$$\bar{\phi}_{NE} = 0 \Rightarrow \frac{\partial \bar{\rho}_N}{\partial t} \geq 0.$$

This implies that negative terms do not contribute to the decrease of density when it is already zero.

6.3. Hyperbolicity

Let us now investigate whether the model (28) is a hyperbolic PDE (as it is the case for the classical LWR but not the general case for multi-directional 2D LWR [40]). Hyperbolicity is a fundamental property determining the behaviour of solutions, which also plays an important role in the choice of the corresponding numerical scheme. For example, if we show that the model is a hyperbolic PDE, then we can apply the Godunov scheme for numerical simulation.

In contrast to other PDE types, in a hyperbolic PDE any disturbance made in the initial data will travels along the characteristics of the equation with a finite propagation speed. Although the definition of hyperbolicity is fundamentally a qualitative one, there are precise criteria using which we can classify a partial differential equation as hyperbolic. In this section, we will apply this criteria to determine hyperbolicity of our model (28). Equation (28) can be written in a following general form:

$$\partial_t \bar{\rho} + \partial_x \big[F^x(\bar{\rho}, x, y)\big] + \partial_y \big[F^y(\bar{\rho}, x, y)\big] = g(\bar{\rho}, x, y), \tag{33}$$

where F^x and F^y are the flow matrices defined from (28) as

$$F^x = \begin{bmatrix} \overline{\cos\theta}_N \bar{\phi}_N & 0 & 0 & 0 \\ 0 & \overline{\cos\theta}_E \bar{\phi}_E & 0 & 0 \\ 0 & 0 & \overline{\cos\theta}_W \bar{\phi}_W & 0 \\ 0 & 0 & 0 & \overline{\cos\theta}_S \bar{\phi}_S \end{bmatrix},$$

and

$$F^y = \begin{bmatrix} \overline{\sin\theta}_N \bar{\phi}_N & 0 & 0 & 0 \\ 0 & \overline{\sin\theta}_E \bar{\phi}_E & 0 & 0 \\ 0 & 0 & \overline{\sin\theta}_W \bar{\phi}_W & 0 \\ 0 & 0 & 0 & \overline{\sin\theta}_S \bar{\phi}_S \end{bmatrix}.$$

The right-hand side term $g(\bar{\rho}, x, y)$ from (33) corresponds to the vector containing all the mixing terms from (28):

$$g(\bar{\rho}, x, y) = \frac{1}{L} \begin{pmatrix} \bar{\phi}_{EN} + \bar{\phi}_{WN} + \bar{\phi}_{SN} - \bar{\phi}_{NE} - \bar{\phi}_{NW} - \bar{\phi}_{NS} \\ \bar{\phi}_{NE} + \bar{\phi}_{WE} + \bar{\phi}_{SE} - \bar{\phi}_{EN} - \bar{\phi}_{EW} - \bar{\phi}_{ES} \\ \bar{\phi}_{NW} + \bar{\phi}_{EW} + \bar{\phi}_{SW} - \bar{\phi}_{WN} - \bar{\phi}_{WE} - \bar{\phi}_{WS} \\ \bar{\phi}_{NS} + \bar{\phi}_{ES} + \bar{\phi}_{WS} - \bar{\phi}_{SN} - \bar{\phi}_{SE} - \bar{\phi}_{SW} \end{pmatrix}.$$

The spatial derivatives of flow matrices from (33) can be written as a chain rule

$$\partial_x \big[F^x(\bar{\rho}, x, y)\big] = \partial_{\bar{\rho}} F^x(\bar{\rho}, x, y) \cdot \partial_x \bar{\rho} + \partial_x F^x(\bar{\rho}, x, y), \quad \text{and}$$
$$\partial_y \big[F^y(\bar{\rho}, x, y)\big] = \partial_{\bar{\rho}} F^y(\bar{\rho}, x, y) \cdot \partial_y \bar{\rho} + \partial_y F^y(\bar{\rho}, x, y),$$

which is further inserted into equation (33) that yields

$$\partial_t \bar{\rho} + \partial_{\bar{\rho}} F^x(\bar{\rho}, x, y) \cdot \partial_x \bar{\rho} + \partial_{\bar{\rho}} F^y(\bar{\rho}, x, y) \cdot \partial_y \bar{\rho} = b(\bar{\rho}, x, y), \tag{34}$$

where $b(\bar{\rho}, x, y) = g(\bar{\rho}, x, y) - \partial_x F^x(\bar{\rho}, x, y) - \partial_y F^y(\bar{\rho}, x, y)$. According to Section 3.1 of [44], the right-hand side part of (34) $b(\bar{\rho}, x, y)$ does not play any significant role for the analysis. Thus, we simply omit it by setting $b(\bar{\rho}) = 0$.

Let us further rewrite (34) as

$$\partial_t \bar{\rho} + A^x \partial_x \bar{\rho} + A^y \partial_y \bar{\rho} = 0, \tag{35}$$

where $A^x = \partial F^x / \partial \bar{\rho}$ and $A^y = \partial F^y / \partial \bar{\rho}$ represent matrices of flow derivatives:

$$A^x = \begin{bmatrix} \overline{\cos\theta}_N \frac{\partial \bar{\phi}_N}{\partial \bar{\rho}} & 0 & 0 & 0 \\ 0 & \overline{\cos\theta}_E \frac{\partial \bar{\phi}_E}{\partial \bar{\rho}} & 0 & 0 \\ 0 & 0 & \overline{\cos\theta}_W \frac{\partial \bar{\phi}_W}{\partial \bar{\rho}} & 0 \\ 0 & 0 & 0 & \overline{\cos\theta}_S \frac{\partial \bar{\phi}_S}{\partial \bar{\rho}} \end{bmatrix},$$

and

$$A^y = \begin{bmatrix} \overline{\sin\theta}_N \frac{\partial \bar{\phi}_N}{\partial \bar{\rho}} & 0 & 0 & 0 \\ 0 & \overline{\sin\theta}_E \frac{\partial \bar{\phi}_E}{\partial \bar{\rho}} & 0 & 0 \\ 0 & 0 & \overline{\sin\theta}_W \frac{\partial \bar{\phi}_W}{\partial \bar{\rho}} & 0 \\ 0 & 0 & 0 & \overline{\sin\theta}_S \frac{\partial \bar{\phi}_S}{\partial \bar{\rho}} \end{bmatrix}.$$

The system (35) is symmetrisable hyperbolic, since matrices A^x and A^y are both symmetric. This implies that the system (35) is hyperbolic [44], which equivalently means that the NEWS model (28) is a hyperbolic PDE system.

7. Validation of NEWS model

This section is devoted to validation of the NEWS model that has been previously derived and analyzed. First, we will discuss the numerical method used to simulate traffic with NEWS model. Then, the similarity measure will be introduced to enable a quantitative comparison of two density distributions. Further, we will compare the density predicted by the numerical simulation of NEWS model (28) with the results predicted by commercial software Aimsun. Finally, we will compare the prediction results with the data obtained from real-life measurements in Grenoble city center.

(a) Google satellite view (b) Network in Aimsun

Figure 8: Selected area in Grenoble downtown.

7.1. Numerical scheme

As a network we take an area located in Grenoble downtown (France) with a total surface of around 1.4×1 km^2, see Fig.8a) for the Google satellite view and Fig.8b) for the network model in Aimsun of this area.

For the numerical simulation of (28), we use the Godunov scheme [22] in two dimensions. We introduce $\Omega \in \mathbb{R}^2$ to be a rectangular continuum domain

capturing the urban network, and $\Omega : [x_{min}, x_{max}] \times [y_{min}, y_{max}]$. We start by defining a numerical grid in $\Omega \times \mathbb{R}^+$ by setting

- n_x to be number of cells to discretize x dimension,
- n_y to be number of cells to discretize y dimension,
- $\Delta x = (x_{max} - x_{min})/n_x$ to be the space cell size in x dimension,
- $\Delta y = (y_{max} - y_{min})/n_y$ to be the space cell size in y dimension,
- Δt to be the time cell size,
- $(i\Delta x, j\Delta y, k\Delta t)$ for $i \in \{1, \dots, n_x\}$, $j \in \{1, \dots, n_y\}$ and $k \in \mathbb{Z}^+$ to be the grid point.

For the simulation of traffic on this area of Grenoble, we set $n_x = 60$ and $n_y = 60$, i.e., the 2D plane is divided into $n_x \times n_y = 3600$ cells. The mesh sizes Δx and Δy and time step Δt are chosen such that they satisfy the Courant-Friedrichs-Lewy condition [45]. The discrete density vector is then $\bar{\rho}^k(i,j) = \left(\bar{\rho}^k_N(i,j), \bar{\rho}^k_E(i,j), \bar{\rho}^k_W(i,j), \bar{\rho}^k_S(i,j)\right)^T$. The density in each direction $q = \{N, E, W, S\}$ is updated for every grid point $\forall (i,j,k) \in \{1, \dots, n_x\} \times \{1, \dots, n_y\} \times \mathbb{Z}^+$ as

$$\bar{\rho}^{k+1}_q(i,j) = \bar{\rho}^k_q(i,j) + \Delta t \Big[E^k_q(i,j) + F^k_{x,q}(i,j) + F^k_{y,q}(i,j) + H^k_q(i,j) \Big],$$

where $E^k_q(i,j)$ corresponds to the mixing term between direction layers

$$\begin{aligned} E^k_q(i,j) = & \frac{1}{L(i,j)} \sum_{\substack{r=1 \\ r \neq q}}^{4} \Big(\min \left\{ \bar{\alpha}_{rq}(i,j) \bar{D}^k_r(i,j), \bar{\beta}_{rq}(i,j) \bar{S}^k_q(i,j) \right\} \\ & - \min \left\{ \bar{\alpha}_{qr}(i,j) \bar{D}^k_q(i,j), \bar{\beta}_{qr}(i,j) \bar{S}^k_r(i,j) \right\} \Big), \end{aligned}$$

and $F^k_{x,q}(i,j)$, $F^k_{y,q}(i,j)$ are the derivative terms computed as

$$\begin{aligned} F^k_{x,q}(i,j) = & \frac{\overline{\cos\theta}_q(i,j) + \overline{\cos\theta}_q(i-1,j)}{2\Delta x} \min \left\{ \bar{D}^k_q(i-1,j), \bar{S}^k_q(i,j) \right\} \\ & - \frac{\overline{\cos\theta}_q(i,j) + \overline{\cos\theta}_q(i+1,j)}{2\Delta x} \min \left\{ \bar{D}^k_q(i,j), \bar{S}^k_q(i+1,j) \right\}, \end{aligned}$$

$$F^k_{y,q}(i,j) = \frac{\overline{\sin\theta}_q(i,j) + \overline{\sin\theta}_q(i,j-1)}{2\Delta y} \min\left\{\bar{D}^k_q(i,j-1), \bar{S}^k_q(i,j)\right\} - \frac{\overline{\sin\theta}_q(i,j) + \overline{\sin\theta}_q(i,j+1)}{2\Delta y} \min\left\{\bar{D}^k_q(i,j), \bar{S}^k_q(i,j+1)\right\}.$$

Notice that $F^k_{x,q}(i,j)$, $F^k_{y,q}(i,j)$ are obtained using the upwind scheme [46] for $\overline{\cos\theta}_q(i,j) > 0$, $\overline{\sin\theta}_q(i,j) > 0$. The upwind scheme is used to guarantee the correct direction of information propagation in a flow field, which needs to be reversed if $\overline{\cos\theta}_q(i,j) < 0$ for $F^k_{x,q}(i,j)$ and $\overline{\sin\theta}_q(i,j) < 0$ for $F^k_{y,q}(i,j)$.

Finally, $H^k_q(i,j)$ includes source and sink terms, thus it is computed as

$$H^k_q(i,j) = \frac{1}{L(i,j)}\Big(\min\left\{\bar{D}^{source,k}_q(i,j), \bar{S}^k_q(i,j)\right\} - \min\left\{\bar{D}^k_q(i,j), \bar{S}^{sink,k}_q(i,j)\right\}\Big).$$

Remark 3. Notice that one the computational time of one simulation step depends linearly on the number of cells $n_x \times n_y$, i.e., $O(n_x n_y)$.

7.2. Structural similarity measure

In order to enable a quantitative comparison between two density distributions, we use the *structural similarity measure* (SSIM) [47]. This should be understood as an index used to measure the similarity between two images. Thereby, three different image properties are compared: luminance, contrast and structure. In general, the SSIM between two density distributions $\bar{\rho}_1(i,j)$ (NEWS prediction) and $\bar{\rho}_2(i,j)$ (reference distribution) $\forall (i,j) \in \{1,\ldots,n_x\} \times \{1,\ldots,n_y\}$ can be calculated as:

$$SSIM(\bar{\rho}_1, \bar{\rho}_2) = \frac{(2\mu_1\mu_2 + c)(2\sigma_{12} + c)}{(\mu_1^2 + \mu_2^2 + c)(\sigma_1^2 + \sigma_2^2 + c)}, \tag{36}$$

where μ_1 and μ_2 are the mean values of distributions $\bar{\rho}_1$ and $\bar{\rho}_2$ over the domain that are computed as:

$$\mu(\bar{\rho}) = \frac{1}{n_x}\frac{1}{n_y}\sum_{q=N}^{S}\sum_{i=1}^{n_x}\sum_{j=1}^{n_y}\bar{\rho}_q(i,j). \tag{37}$$

This term is used to compare luminance of two images. Then, σ_1 and σ_2 in (36) are the standard deviations of density distributions used to compare the signal contrasts:

$$\sigma(\bar{\rho}) = \sqrt{\frac{1}{n_x}\frac{1}{n_y}\sum_{i=1}^{n_x}\sum_{j=1}^{n_y}\left(\sum_{q=N}^{S}\bar{\rho}_q(i,j) - \mu(\bar{\rho})\right)^2},$$

and σ_{12} is the correlation coefficient of two density distributions used to measure the similarity of their structures:

$$\sigma(\bar{\rho}_1, \bar{\rho}_2) = \frac{1}{n_x}\frac{1}{n_y}\sum_{i=1}^{n_x}\sum_{j=1}^{n_y}\left(\sum_{q=N}^{S}\bar{\rho}_{q,1}(i,j) - \mu_1\right)\left(\sum_{q=N}^{S}\bar{\rho}_{q,2}(i,j) - \mu_2\right).$$

Finally, $c > 0$ in (36) is a constant that needs to be small, e.g., we take $c = 1 \cdot 10^{-13}$ for the computation. This constant prevents instability, when the denominator is close to zero. The range of SSIM is $[-1, 1]$, where 1 is achieved if two images are identical, whereas -1 means that one image is the inverse of the second image.

The main advantage of using SSIM is that it is a perception-based metric used to detect structural changes in the image, while, for example, the mean square error evaluates only the absolute error rather than differences in congestion patterns. Thus, even if two density distributions are characterized to have the same number of cars, the SSIM is still able to detect whether congested zones have different shapes.

7.3. Model validation with Aimsun

We run a scenario of congestion formation in the selected area of Grenoble downtown (see Fig. 8). For this, we use microsimulator Aimsun and perform also a numerical simulation of traffic density governed by the NEWS model (31). For the numerical simulation we deploy the 2D Godunov scheme (see Sec. 7.1), and then obtained steady states are compared. Aimsun takes network, turning ratios and inflows as input, and produces microsimulations of vehicle trajectories. We then reconstruct the density distribution from vehicle positions predicted by Aimsun and compare it to the state predicted by NEWS model.

In general, we have access to the following network data: (x, y) coordinates of all intersections and its corresponding roads, as well as speed limits and number of lanes for each road. Using these data, we compute the parameters of the fundamental diagram $\bar{v}$, $\bar{\omega}$, $\bar{\rho}_{max}$ and the intersection parameters $\bar{\alpha}$, $\bar{\beta}$, L, $\overline{\cos\theta}$, $\overline{\sin\theta}$ in the NEWS framework for all the intersections as follows. For each road

j in the selected Grenoble area, we read the free-flow velocity v_j from its speed limit data. The maximal density $\rho_{max,j}$ is computed by placing a car every 6 m at every road, and then the Kernel Density Estimation method (KDE) is applied. This method is used to estimate densities from vehicle positions. It is assumed that every car represents the center of a Gaussian kernel, and it contributes to the total density within the radius set by the standard deviation of the Gaussian function (here we assume it to be 70 m). Further, we also assume $\rho_{c,j} = \rho_{max,j}/3$ since it approximately corresponds to the estimated value from the measurement data for this area of Grenoble [48]. This in turn allows us to calculate the negative kinematic wave speed ω_j and road capacities $\phi_{max,j}$ from the triangular FD shape. Then, these parameters are translated into NEWS formulation using the network geometry, see Sec. 4.4 for more details.

In order to determine the traffic flow direction, we use turning ratios α_{ij} for each road i towards road j that are estimated as

$$\alpha_{ij} = \frac{\phi_{max,j}}{\sum_{q=1}^{n_{out}} \phi_{max,q}}.$$

Then, supply ratios β_{ij} are calculated using (7). Both ratios α and β are translated into NEWS formulation as in (17) and (18). Further, coordinates of road's both ends are used to determine its length l_j and orientation angle θ_j, from which we then obtain L, $\overline{\cos\theta}$, $\overline{\sin\theta}$ in NEWS formulation as described in Sec. 5.2.

Then all these intersection and FD parameters are approximated for every grid point $(i, j) \in \{1, \dots, n_x\} \times \{1, \dots, n_y\}$ using Inverse Distance Weighting method as described in Sec. 5.3. In general, low values of weighting parameter η from (29) imply that only the global trend of the density propagation is reproduced, while high values of η imply that the location of real roads is more emphasized (see [38] for more details). For the results presented in this section, we chose $\eta = 20$, which is a relatively low value.

First of all, we load the Grenoble network to Aimsun (see Fig.8b)), and let vehicles enter through its boundaries by specifying inflows. We choose inflows such that the main stream of vehicles comes from the South of the area. The

microsimulations evolve for 2.5 min, and then the state is saved and later used as an initial condition for both Aimsun and numerical simulation of the NEWS model. Afterwards, we continue the microsimulation on Aimsun until we do not perceive any structural changes in the state, which indicates that a steady state has been achieved. The results are saved as vehicle positions at all time instants. We use the density reconstruction procedure to be able to transform the standard Aimsun data into a density distribution (KDE, see the details above and also [38]). KDE in 1D is also used to smooth inflows such that they enter the domain in a continuous line rather than at discrete points of space. We set constant inflows at network boundaries in order to let the system converge to a steady state, since steady states are easier to compare. We then perform a numerical simulation of the NEWS model as described in Sec. 7.1 using the initial conditions from Aimsun.

The results are depicted in Figure 9, where the comparison of both density distributions is shown for $t \in [0, 50]$ min. We see that in both cases the distributions look quite similar but not identical, which might be caused by several things. In Aimsun, vehicles are restricted to move only on real physical roads, while more freedom of movement is perceived in a PDE-driven system. Moreover, in Aimsun, turning ratios indicate the probability with which a car turns to one or another road, whenever it reaches an intersection at some time instant. Thus, turning ratios in Aimsun should be understood as mathematical expectation rather than deterministic values. Hence, it often appears that scenarios in Aimsun, although having the same initial condition and inflows, converge to different density distributions. Vehicles might get stuck in different parts of the city, while this is unlikely to happen during the numerical simulation of NEWS density, where cars move on a continuum domain. However, on a global scale traffic regimes seem to be reproduced correctly in most parts of the city.

Let us now compute the structural similarity measure (36) to compare two density distributions from Fig. 9. For that the domain is divided into 9 windows of equal size, as drawn in Fig. 10a). We do this in order to be able to compare density distributions zone-by-zone. Zones are numbered from top left to bottom

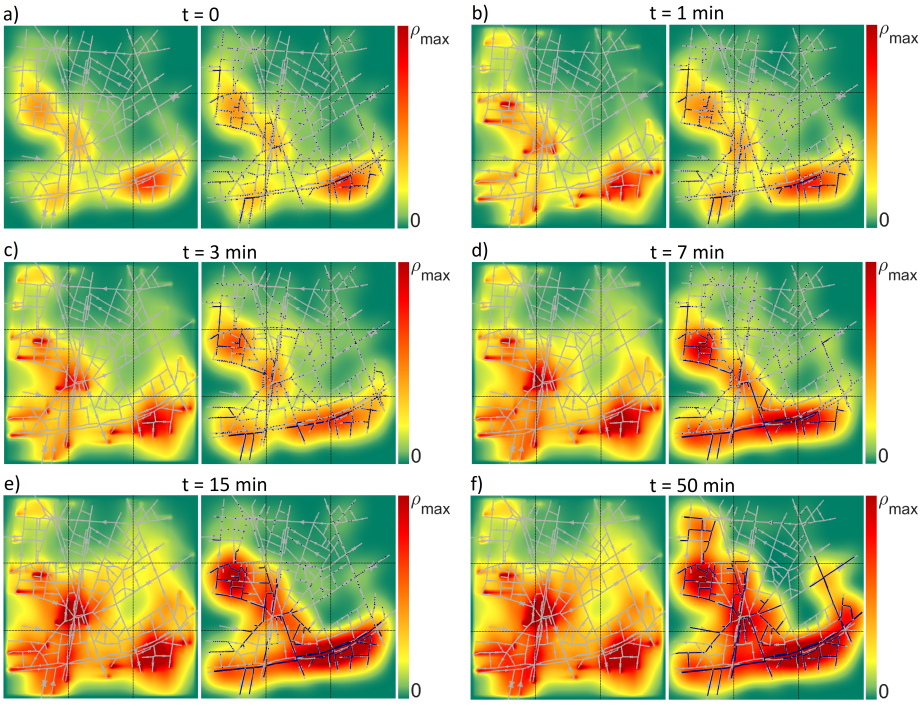

Figure 9: Congestion formation in Grenoble downtown for $t \in [0, 50]$ min: numerical simulation of density governed by NEWS model (left plots) and Aimsun (right plots). Weighting parameter $\eta = 20$. Blue dots denote vehicle positions in Aimsun. Black dashed lines separate Grenoble in zones used for the calculation of SSIM.

right, as shown in Fig. 10a). The SSIM of the whole domain is then calculated as the mean value over all zones:

$$\overline{SSIM}(\bar{\rho}_1, \bar{\rho}_2) = \frac{\sum_{l=1}^{N_{zones}} SSIM_l \; \mu_l(\bar{\rho}_2)}{\sum_{l=1}^{N_{zones}} \mu_l(\bar{\rho}_2)}, \tag{38}$$

where $N_{zones} = 9$ is the total number of zones in the domain, $SSIM_l$ is referred to zone l each given by (36), and $\mu_l(\bar{\rho}_2)$ is the corresponding weight of the zone based on its occupancy level in the reference distribution (here $\bar{\rho}_2$ is the total density in Aimsun). Thus, the fewer cars a zone has, the smaller is its weight. The weights are assigned in order to avoid giving too much importance to zones that are currently almost empty. Notice that $\mu_l(\bar{\rho}_2(t))$ is a time-dependent parameter.

In its original formulation, SSIM values range from -1 to 1. In order to facilitate the interpretation of this index in the context of density comparison, we make its range to be $SSIM \in [0, 1]$ by doing $(SSIM + 1)/2$. Thus, $SSIM = 1$ implies that two distributions are identical, and $SSIM = 0$ means that one distribution is completely the opposite of the second one (inverted image).

The SSIM of corresponding zones in both distributions is depicted as a function of time in Fig. 10b). It seems that the most problematic zones are the most empty ones that are concentrated in the upper part of the domain (zones 2 and 3), while the best captured zones are the most congested ones (zones 4 and 9). This can be explained by the fact that the main stream of vehicles enters the domain from the South (as prescribed by the boundary conditions in our scenario), where they build the most congested areas. Thus, cars might not have reached the upper part in Aimsun, since they got stuck in the Southern part of the area.

Finally, in order to unable a quantitative comparison of the density in the whole Grenoble area, the SSIM is averaged over all zones by using (38), and we obtain the result depicted in Fig.11. Thereby, we can see that the overall SSIM is approximately equal to 0.9 ($\approx 90\%$ accuracy), which indicates that the

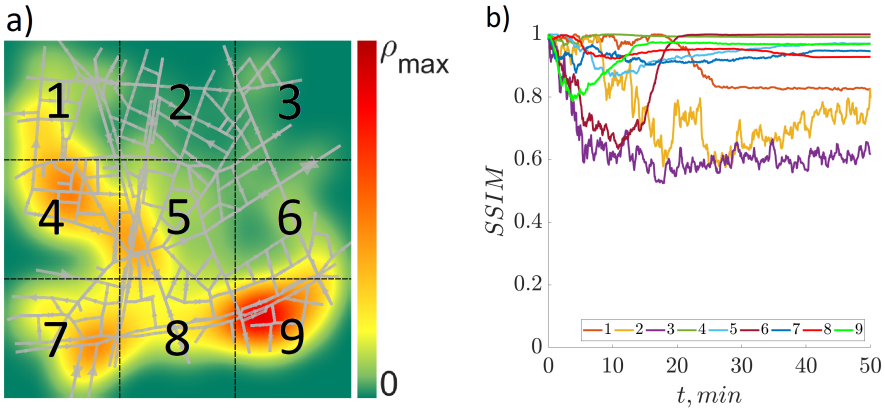

Figure 10: a) Zone numbering in Grenoble network, b) structural similarity zone-by-zone: $SSIM_l$ with $l = \{1, \ldots, 9\}$.

congested steady state is close to be reproduced correctly by the NEWS model (28).

7.4. Model validation with real data

For the model validation with real data, we make use of Grenoble Traffic Lab for Urban Networks known as GTL Ville, see `http://gtlville.inrialpes.fr/`. This is an experimental platform for real-time collection of traffic data coming from a network of stationary flow sensors installed in Grenoble downtown, see Fig. 12. This platform also provides real-time traffic indicators oriented towards the users of the city, traffic operators and researchers [49]. The collected data and computed indicators are available for download at the GTL website. Note that the real data is referred to density values estimated from measured flows rather then ground true traffic density (see below for more details).

The maximal densities at every road $\rho_{max,j}$, capacities $\phi_{max,j}$, road lengths l_j and orientations θ_j are the same as described above, since these parameters are defined by the network topology, which remains the same for the real-life experiment. However, the free-flow speed data are now taken from floating car data reported from several vehicles that are equipped with devices such as a GPS navigator. The free-flow speed is estimated as the maximal speed of a vehicle in the absence of other cars, and it starts decreasing as the density of

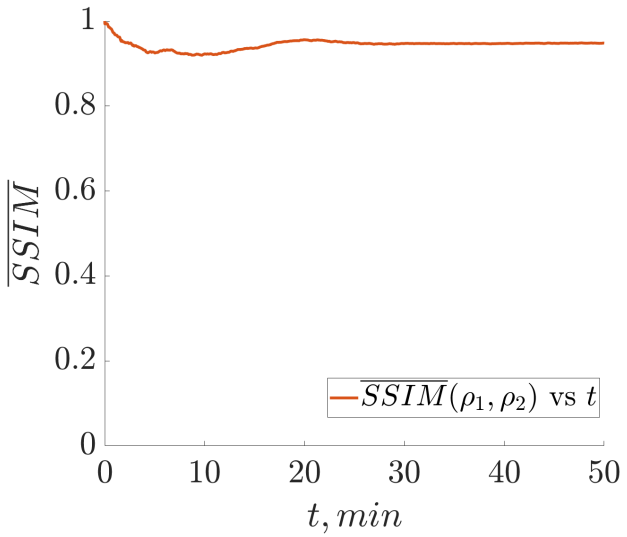

Figure 11: Mean value over zones of $\overline{SSIM}$ computed by (38) between densities obtained with Aimsun and numerical simulation of NEWS as a function of time.

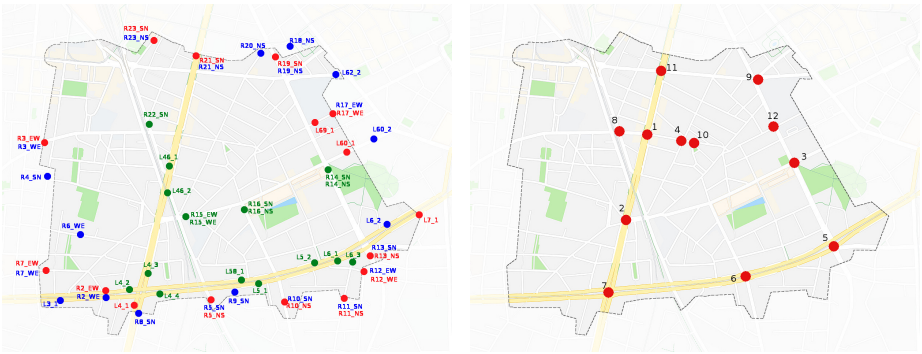

(a) Fixed sensors (b) Bluetooth devices

Figure 12: Sensor location in Grenoble downtown: (a) fixed flow sensors: R denote radars and L denote induction loops; (b) automatic vehicle identifiers using Bluetooth installed at 12 intersections of Grenoble during a measurement campaign lasting for one week. These figures are taken from [48].

surrounding cars increases. It is worth noting that, in general, the free-flow speed is lower than the corresponding speed limit value, since in reality cars lose their average velocity, e.g., by stopping at traffic lights.

Now let us explain how do we get turning ratios α_{ij}. These data are obtained from automatic vehicle identifiers using Bluetooth devices that were installed at adjacent incoming and outgoing roads of 12 intersections in total, see their location in Fig.12b). These identifiers are able to detect vehicles equipped with another Bluetooth device, which enables to assign origin and destination road of individual vehicles. For the estimation of the remaining turning ratios (since there are more than 12 intersections in total), the information on road importance is used (historical data), and then the optimization problem minimizing the deviation of predicted and actual flows is solved.

Finally, we also get the estimated density values for every road ρ_j for every minute of the 8th of January 2021 from 6 am to 9 pm, as well as inflows and outflows at domain boundaries. Notice that in this scenario inflows are time-dependent functions. Estimation of free-flow speed, turning ratios, vehicle density and boundary flows is described in more details in [50].

In Fig. 12a) the sensors marked in blue are those giving boundary inflows and red sensors give boundary outflows. Sensors marked in green were used for the validation of state estimation procedure. Notice that the state estimation procedure is not free of error and it does not reconstruct the state exactly, since there are only a limited number of sensors due to economical cost.

In order to get density values all over the continuum plane, i.e., at every point in Grenoble downtown (not only at roads), we divide each road into 10 parts, and at the boundary between each part we virtually place a group of vehicles. We then assume that all these cars contribute to the global density around 70 m from its positions KDE method. We also use KDE for the inflow values, as it was done in the previous example.

The results are depicted in Fig. 13, where the comparison of two density distributions is shown. We again see that in both cases the distributions look quite similar. The first possible reason for these distributions to be non-identical

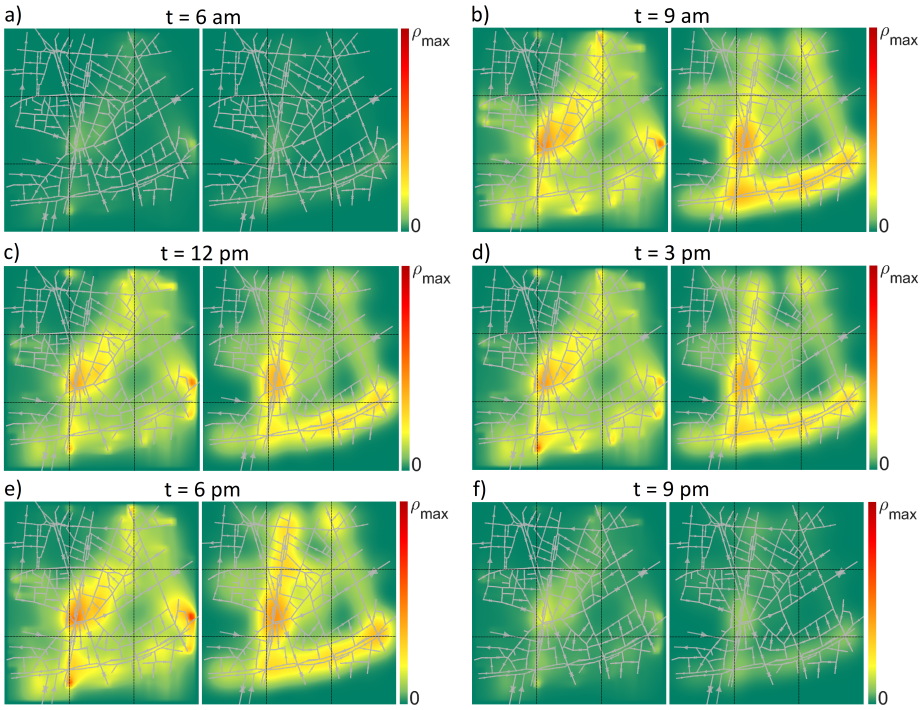

Figure 13: Evolution of traffic density in Grenoble downtown on 8th of January 2021 from $t = 6$ am to $t = 9$ pm: numerical simulation of NEWS model (left plots) and density estimated from sensor data (right plots). Weighting parameter $\eta = 20$.

is the probabilistic nature of turning ratios in reality opposed to deterministic nature in numerical simulation. Another reason is that the NEWS model does not include traffic lights, as well as it is not able to capture accidents or the effect of pedestrians crossing a road. Moreover, the NEWS model does not take into account parking lots. Thus, in reality parking vehicles are seen as stationary objects that do not contribute to the traffic flow any more, while in NEWS-driven system these vehicles stay in the domain and create congestions, since NEWS model is a conservation law.

Another source of mismatch could be induced by data on inflows and outflows. The problem is that the data represent measured flows in the city that we can not enforce in our system, since there is always a demand-supply problem

that needs to be solved, i.e.,

$$\phi^{source} = \min\left\{D_{ext}, S(\rho)\right\}, \quad \phi^{sink} = \min\left\{D(\rho), S_{ext}\right\},$$

where ext is used in the subscript to highlight that these functions depend on what happens outside the domain. Thus, the available data are not related to demand and supply at domain boundaries but to actual inflow $\hat{\phi}^{source}$ and outflow $\hat{\phi}^{sink}$ of the system (hats are used to denote the measurement data).

To understand which problems can be provoked by these issues, let us consider some measured outflow $\hat{\phi}^{sink}$, which in turn is also just a result of solving the minimum between demand and supply, i.e.,:

$$\hat{\phi}^{sink} = \min\left\{D(\hat{\rho}), S_{ext}\right\}, \tag{39}$$

where demand $D(\hat{\rho})$ depends on the measured density, which might be different from the one we get from the numerical simulation of NEWS-driven density.

For the numerical simulation, the best thing we can do with the measured outflow data $\hat{\phi}^{sink}$ is to use it as a supply of the external area:

$$\phi^{sink} = \min\left\{D(\rho), \hat{\phi}^{sink}\right\}. \tag{40}$$

However, it follows from (39) that $\hat{\phi}^{sink} \leq S_{ext}$, where the equality holds in case of congested traffic. If the traffic is not congested, then setting our external supply to be equal to measured outflow might lead to blocking vehicles at domain exit instead of letting them come out.

Two distributions are again compared by using the weighted SSIM averaged over 9 zones as in the previous case using (38) and (36). The result is depicted in Fig. 14a), while Fig. 14b) is referred to SSIM for each zone computed using (36). Notice that the zone numbering here is the same as in Fig. 10a). The worst captured zones are 1 and 2 located in the upper part of the city, and the best results are achieved for zones 5, 4 and 8. A possible reason might be the fact that vehicles get stuck at the bottom of the city in the real experiment, while they more freely in a PDE-governed system. In general, notice that the best results are achieved for the time when the congestion level is the highest,

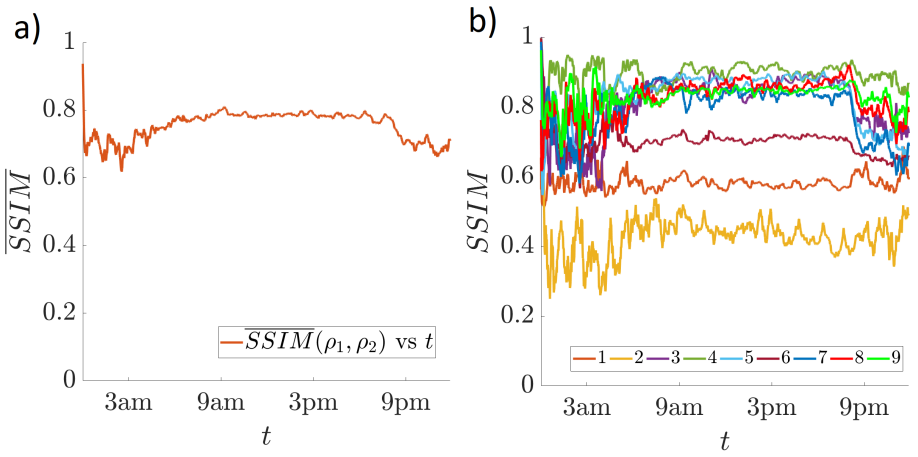

Figure 14: a) Mean $\overline{SSIM}$ (38) between the density ρ_1 predicted by numerical simulation of NEWS model and the density ρ_2 estimated from real data as a function of time, b) similarity zone-by-zone: $SSIM_l$ with $l = \{1, \ldots, 9\}$.

as we can see from Fig. 14a). This is related to the weighting parameters used for calculation of SSIM (38). Weights tend to introduce more noisiness into computation, when there are only a few cars in the city. Finally, recall that the real-life data are also an approximation, since these densities are obtained by the estimation procedure that is not error-free due to the lack of sensors at every road. On average, the total SSIM is almost 0.8 (80% accuracy), which indicates that two density distributions are still quite close.

It is worth noting that the source code used for model validation is an *open source* project that you can find here: `https://github.com/Lyurlik/multidirectional-traffic-model`, see also Appendix for more details.

8. Conclusions

To summarize, we have derived a macroscopic continuous model for urban traffic that consists of 4 PDEs, which makes it suitable for explicit analysis. It is scalable and does not change its form as the size of urban network grows. This model can be used to predict traffic evolution on urban networks of arbitrary size, although we have demonstrated its performance on a relatively small

network of Grenoble downtown. The derivation was done analytically using the demand-supply concept at one intersection, which lets us conclude that the obtained model can be seen as extension of the kinematic wave theory (LWR) for general multi-directional networks. During the derivation, we had to make two assumptions on network structure: it is especially well-suitable 1) for networks that are well-designed in terms of maximal flows (27), and 2) if network roads are in the same traffic regime. These assumptions were needed to obtain a PDE-based model out of the ODE network model. Therefore, the NEWS model might be less exact than the network-based model, which represents its main limitation.

The propagation of traffic flow in each direction is driven by the demand-supply concept that uses a fundamental diagram (that can be any concave flow-density relation) whose parameters are determined by network topology, as well as by data from real-life experiments. Moreover, vehicles moving in some direction layer can switch to another layer, i.e., there exists a mixing between different direction layers, which is an important aspect to be included into the model due to its physical ubiquity.

We have been able to show that NEWS model is a hyperbolic PDE system. Hyperbolicity implies that a lot of analysis tools used for hyperbolic conservation laws (such as LWR) can be also used to analyse the structure of NEWS, which significantly simplifies analysis for future tasks such as explicit control design or estimation of steady states. The model prediction results have been validated using experimental platform GTL Ville that provides real-time data from a network of sensors installed in Grenoble. This project is an open source such that the results are reproducible and can be used for future studies.

As a promising direction for the future development of optimally operating transportation systems, it would be interesting to use this model to solve traffic control tasks on urban networks such as vehicle density stabilization around some desired equilibrium value, e.g., throughput maximization.

Appendix A. List of notations

Appendix A.1. Road formulation

Variable	Meaning	Units
$\rho(x, y, t)$	vehicle density	veh/m
$\Phi(x, y, \rho)$	flow function	veh/s
$v(x, y)$	kinematic wave speed in free-flow regime	m/s
$\omega(x, y)$	kinematic wave speed in congested regime	m/s
$\rho_c(x, y)$	critical vehicle density	veh/m
$\phi_{max}(x, y)$	flow capacity	veh/s
$D(\rho)$	demand function	veh/s
$S(\rho)$	supply function	veh/s
ϕ_i^{in}	inflow to intersection from road i	veh/s
ϕ_j^{out}	outflow from intersection to road j	veh/s
ψ_j^{in}	inflow into road j	veh/s
ψ_j^{out}	outflow from road j	veh/s
n_{in}	number of incoming roads for intersection	-
n_{out}	number of outgoing roads from intersection	-
ϕ_{ij}	flow from road i to road j	veh/s
α_{ij}	turning ratio from road i to road j	-
β_{ij}	supply coefficient of road j for the flow from road i	-
D_{ij}	flow demand of road i to enter road j	veh/s
S_{ij}	supply of road j for flow coming from road i	veh/s
θ_i	angle that road i builds with East	degrees
l_i	length of road i	m

Variable	Meaning	Units
$p_\theta^N, p_\theta^S, p_\theta^W, p_\theta^E$	projection coefficients wrt corresponding directions	-
$P_{in} \in \mathbb{R}^{4\times n_{in}}$	projection matrix for incoming roads into NEWS	-
$P_{out} \in \mathbb{R}^{4\times n_{out}}$	projection matrix for outgoing roads into NEWS	-
$\bar{\rho}(x,y,t)$	4-dim density vector	veh/m
$\bar{\Phi}(x,y,\bar{\rho})$	4-dim flow function	veh/s
$\bar{\rho}_{max}(x,y)$	4-dim maximal density	veh/m
$\bar{v}(x,y)$, $\bar{\omega}(x,y)$	4-dim kinematic wave speeds	m/s
$\bar{\rho}_c(x,y)$	4-dim critical density	veh/m
$\bar{\phi}_{max}(x,y)$	4-dim flow capacity	veh/s
$\bar{D}(x,y,\bar{\rho})$	4-dim demand function	veh/s
$\bar{S}(x,y,\bar{\rho})$	4-dim supply function	veh/s
$\bar{\phi}_N^{in}(x,y)$	inflow into intersection in the North direction	veh/s
$\bar{\phi}_N^{out}(x,y)$	outflow from intersection in the North direction	veh/s
$\bar{\phi}_{NE}(x,y)$	partial flow from North to East wrt intersection	veh/s
$\bar{\psi}_N^{in}(x,y)$	inflow into outgoing road in the North direction	veh/s
$\bar{\psi}_N^{out}(x,y)$	outflow from outgoing road in the North direction	veh/s
$\bar{\psi}_{NE}(x,y)$	partial flow from North to East wrt outgoing roads	veh/s
$\bar{\alpha}_{EN}(x,y)$	turning ratio from East to North layer	-
$\bar{\beta}_{EN}(x,y)$	supply of East layer for the flow from the North	-
$\overline{\cos\theta}(x,y)$, $\overline{\sin\theta}(x,y)$	average direction parameters of intersection	-
$L(x,y)$	average length of outgoing roads of intersection	m

Appendix B. Proof that $\bar{\psi}_N = \min\{\bar{D}_N, \bar{S}_N\}$

Here we prove that the flow in some direction (here North) can be written as a function of demand and supply of the same direction:

$$\bar{\psi}_N = \min\left\{\bar{D}_N, \bar{S}_N\right\},$$

which allows to simplify the model (24).

Let us consider $(1-\gamma)\bar{\psi}_{EN} + \gamma\bar{\psi}_{NE}$ from (25). By definition (16) we get:

$$\bar{\psi}_{EN} = \min\left\{\bar{\alpha}_{EN}\bar{D}_E, \bar{\beta}_{EN}\bar{S}_N\right\}, \quad \bar{\psi}_{NE} = \min\left\{\bar{\alpha}_{NE}\bar{D}_N, \bar{\beta}_{NE}\bar{S}_E\right\}.$$

Notice that now we omit indices "in" and "out" in the demand and supply functions, since they are now referred to the same point. This comes from the continuation, due to which intersections are now assumed to be infinitesimally small in space.

Recall that by definition of the demand-supply formulation, if $\bar{D}_E < \bar{\psi}_{max,E}$, then $\bar{S}_E = \bar{\psi}_{max,E}$ and vice versa. The same holds for $\bar{D}_N$ and $\bar{S}_N$. For simplicity of writing denote $Q(\gamma) = (1-\gamma)\bar{\psi}_{EN} + \gamma\bar{\psi}_{NE}$. We will prove that there always exists γ such that $Q(\gamma) = \min\left\{\bar{\alpha}_{NE}\bar{D}_N, \bar{\beta}_{EN}\bar{S}_N\right\}$. There are no more than six different possibilities:

1. $\bar{\alpha}_{EN}\bar{D}_E < \bar{\beta}_{EN}\bar{S}_N$ and $\bar{\alpha}_{NE}\bar{D}_N > \bar{\beta}_{NE}\bar{S}_E$. From the first inequality we obtain

   $$\bar{\alpha}_{EN}\bar{D}_E < \bar{\beta}_{EN}\bar{S}_N \leq \bar{\beta}_{EN}\bar{\psi}_{max,N} = \bar{\alpha}_{EN}\bar{\psi}_{max,E},$$

   where the last equality comes for the assumption that the network is well-designed (27). Thus, we get that

   $$\bar{D}_E < \bar{\psi}_{max,E}.$$

   From the other side, if we consider the second inequality, we get

   $$\bar{\beta}_{NE}\bar{S}_E < \bar{\alpha}_{NE}\bar{D}_N \leq \bar{\alpha}_{NE}\bar{\psi}_{max,E} \Rightarrow \bar{S}_E < \bar{\psi}_{max,E}.$$

   According to the demand-supply formulation, it is however not possible that $\bar{D}_E < \bar{\psi}_{max,E}$ and $\bar{S}_E < \bar{\psi}_{max,E}$ hold at the same time. Thus, this case can be excluded from consideration.

2. $\bar{\alpha}_{EN}\bar{D}_E > \bar{\beta}_{EN}\bar{S}_N$ and $\bar{\alpha}_{NE}\bar{D}_N < \bar{\beta}_{NE}\bar{S}_E$. This case is also impossible, since from the first inequality we get $\bar{S}_N < \bar{\psi}_{max,N}$ and from the second inequality we get $\bar{D}_N < \bar{\psi}_{max,N}$, which violates the demand-supply formulation.

3. $\bar{\alpha}_{NE}\bar{D}_N \leq \bar{\beta}_{NE}\bar{S}_E$ and $\bar{\alpha}_{NE}\bar{D}_N \leq \bar{\beta}_{EN}\bar{S}_N$. In this case taking $\gamma = 1$ results into

$$Q(1) = \bar{\psi}_{NE} = \min\left\{\bar{\alpha}_{NE}\bar{D}_N, \bar{\beta}_{NE}\bar{S}_E\right\} = \bar{\alpha}_{NE}\bar{D}_N,$$

which in combination with the second inequality yields

$$Q(1) = \min\left\{\bar{\alpha}_{NE}\bar{D}_N, \bar{\beta}_{EN}\bar{S}_N\right\},$$

which is the desired property achieved with $\gamma = 1$.

4. $\bar{\alpha}_{EN}\bar{D}_E \leq \bar{\beta}_{EN}\bar{S}_N$, $\bar{\alpha}_{NE}\bar{D}_N \leq \bar{\beta}_{NE}\bar{S}_E$ and $\bar{\alpha}_{NE}\bar{D}_N > \bar{\beta}_{EN}\bar{S}_N$.
By the first inequality for $\gamma = 0$ we obtain the following:

$$\begin{aligned} Q(0) = \bar{\psi}_{EN} &= \min\left\{\bar{\alpha}_{EN}\bar{D}_E, \bar{\beta}_{EN}\bar{S}_N\right\} \\ &= \bar{\alpha}_{EN}\bar{D}_E \leq \bar{\beta}_{EN}\bar{S}_N. \end{aligned}$$

By the second inequality for $\gamma = 1$ we obtain

$$Q(1) = \bar{\psi}_{NE} = \min\left\{\bar{\alpha}_{NE}\bar{D}_N, \bar{\beta}_{NE}\bar{S}_E\right\} = \bar{\alpha}_{NE}\bar{D}_N,$$

and from the third inequality we get

$$Q(1) > \bar{\beta}_{EN}\bar{S}_N.$$

Combining these results all together, we show the desired property:

$$\begin{cases} Q(0) \leq \bar{\beta}_{EN}\bar{S}_N, \ \Rightarrow \exists\gamma \in [0,1): \ Q(\gamma) = \bar{\beta}_{EN}\bar{S}_N = \\ Q(1) > \bar{\beta}_{EN}\bar{S}_N, \qquad\qquad\qquad\qquad \min\left\{\bar{\alpha}_{NE}\bar{D}_N, \bar{\beta}_{EN}\bar{S}_N\right\}. \end{cases}$$

5. $\bar{\alpha}_{EN}\bar{D}_E \leq \bar{\beta}_{EN}\bar{S}_N$, $\bar{\alpha}_{NE}\bar{D}_N \leq \bar{\beta}_{NE}\bar{S}_E$ and $\bar{\alpha}_{NE}\bar{D}_N \leq \bar{\beta}_{EN}\bar{S}_N$. The analysis here is the same as in case (3): we take $\gamma = 1$, which results in $Q(1) = \min\left\{\bar{\alpha}_{NE}\bar{D}_N, \bar{\beta}_{NE}\bar{S}_N\right\}$.

6. $\bar{\alpha}_{EN}\bar{D}_E \geq \bar{\beta}_{EN}\bar{S}_N$, $\bar{\alpha}_{NE}\bar{D}_N \geq \bar{\beta}_{NE}\bar{S}_E$ and $\bar{\alpha}_{NE}\bar{D}_N > \bar{\beta}_{EN}\bar{S}_N$. Here we also proceed as in case (4): taking $\gamma = 0$ results in $Q(0) = \bar{\beta}_{EN}\bar{S}_N$. Further, by the second condition $Q(1) \leq \bar{\alpha}_{NE}\bar{D}_N$, therefore there exists $\gamma \in [0,1]$ such that $Q(\gamma) = \min\left\{\bar{\alpha}_{NE}\bar{D}_N, \bar{\beta}_{EN}\bar{S}_N\right\}$.

Therefore, if we assume that we can manipulate gamma independently for every pairwise flow, we can summarize the discussion above in the following formula: $(1-\gamma)\bar{\psi}_{EN} + \gamma\bar{\psi}_{NE} = \min\left\{\bar{\alpha}_{NE}\bar{D}_N, \bar{\beta}_{EN}\bar{S}_N\right\}$. This leads to the following transformation of (25):

$$\begin{aligned}\bar{\psi}_N = \bar{\psi}_{NN} + \min\left\{\bar{\alpha}_{NS}\bar{D}_N, \bar{\beta}_{SN}\bar{S}_N\right\} + \\ + \min\left\{\bar{\alpha}_{NW}\bar{D}_N, \bar{\beta}_{WN}\bar{S}_N\right\} + \min\left\{\bar{\alpha}_{NE}\bar{D}_N, \bar{\beta}_{EN}\bar{S}_N\right\}.\end{aligned}$$

Finally, using once again the approximation, where we replace the sum of minima with the minimum of sums, we can write

$$\begin{aligned}\bar{\psi}_N = \min\{\bar{\alpha}_{NN}\bar{D}_N + \bar{\alpha}_{NS}\bar{D}_N + \bar{\alpha}_{NW}\bar{D}_N + \bar{\alpha}_{NE}\bar{D}_N, \\ \bar{\beta}_{NN}\bar{S}_N + \bar{\beta}_{SN}\bar{S}_N + \bar{\beta}_{WN}\bar{S}_N + \bar{\beta}_{EN}\bar{S}_N\} = \min\left\{\bar{D}_N, \bar{S}_N\right\},\end{aligned}$$

which is exactly the property we wanted to prove (26).

Appendix C. Reproducibility of the results

Validation of NEWS model with real data is an *open source* project that was made available for general public here: `https://github.com/Lyurlik/multidirectional-traffic-model`. The README.md file contains all the essential information about the code structure and the data files such that anyone can get use of it for different purposes. Thus, the results are made to be reproducible.

This code is used to produce two different vehicle density distributions: the one predicted by numerical simulation of NEWS model (28), and the other density is the one reconstructed from data obtained from real sensors.

In order to run the code, you need to have the following files:

Network topology

1. *"../ModelValidation/IntersectionTable.csv"* – contains information about intersections: x and y coordinates of every intersection (columns 1 and 2), its `ID` (column 3) and whether it is a node on border (column 4), which means that this intersection is located at domain's boundary through which vehicles may enter (inflows), or exit (outflows);

2. *"../ModelValidation/RoadTable.csv"* – contains information about roads: `ID1` and `ID2` (columns 3 and 4) are the id's of corresponding intersections that the road is connecting, `ID_road` (column 5) is the road's ID, `max_vel` (column 6) is its free-flow limit estimated from real measurements, then we have number of lanes (column 7) and road's length (column 8);
3. *"../ModelValidation/TurnTable.csv"* – contains turning ratios between any pair of roads: `ID1` of incoming road (column 1), `ID2` of outgoing road (column 2) and the turning ratio between these roads (column 5).

Data from real sensors

5. *"../ModelValidation/Timestamp.csv"*– contains time in seconds at which the data are given (unix timestamp), the time step equals to one minute;
6. *"../ModelValidation/Density.csv"* – contains estimated density from real sensors: first number is `road_id` followed by its density (that is assumed to be constant within one road) at all time instants, then the next `road_id` with its density data for each time instant and so on;
7. *"../ModelValidation/AllInflows.csv"* – contains inflow values (in veh/hour) for every road for every time step (one minute). If road is outgoing from intersection that is not on border, then the inflow value is zero;
8. *"../ModelValidation/AllOutflows.csv"* – contains outflow values (in veh/hour) for every road for every time step (one minute). If road is incoming into intersection that is not on border, then the outflow value is zero.

Code structure

The main file of the project is **mainwindow.cpp**: in its constructor we specify the file names to be loaded, start simulation starting time (line 26) and simulation step size (line 28). The paths to files containing network and density data are also specified here. We can also change there the weighting parameter η used to approximate parameters for every cell (line 4), and parameter d_0 (line 5) is used for Gaussian Kernel estimation.

Other important classes are:

- **UrbanNetwork**, which contains all the network geometry information (this is where all the network files are read). This network is used for both densities. In its function *loadRoads*, one needs to specify the minimum distance between the heads of two consequential vehicles.

- **NEWSmodel**, which contains translation procedure of all network and intersection parameters into NEWS-formulation (function *processIntersections*). After all parameters are defined in NEWS, it calls *constructInterpolation* function that approximates these parameters defined for every intersection to be defined on every cell of a network. Then update is performed, where the Godunov numerical scheme is applied for the state update using NEWS model. There is also a function *getSSIMDiff_mean_weighted* used to compute the weighted SSIM index between two densities (38).

- **GrenobleData**, where all the data estimated from the real-life experiments are loaded. In function *reconstructDensity* the density initially given for each road is defined for every cell. Thereby, every road is divided in 10 parts and density values are presented as points on the border between these parts. Then Gaussian Kernel estimation is used to determine density for every cell in the domain.

- **TrafficSystem**, which implements concurrent thread for parallel NEWS simulation relative to the main visualization thread.

Acknowledgment

The Scale-FreeBack project has received funding from the European Research Council (ERC) under the European Unions Horizon 2020 research and innovation programme (grant agreement N 694209).

References

[1] J. M. Lighthill, G. Whitham, On kinematic waves, ii: A theory of traffic flow on long crowded roads, Proc. R. Soc. Lond. A 229 (1955) 317–345. doi:10.1098/rspa.1955.0089.

[2] P. Richards, Shock waves on the highway, Operations Research 47 (1) (1956) 42–51. doi:10.1287/opre.4.1.42.

[3] B. D. Greenshields, J. R. Bibbins, W. S. Channing, H. H. Miller, A study of traffic capacity, Highway Research Board proceedings 1935.

[4] F. van Wageningen-Kessels, H. van Lint, K. Vuik, S. Hoogendoorn, Genealogy of traffic flow models, EURO Journal on Transportation and Logistics 4 (4) (2015) 445–473. doi:https://doi.org/10.1007/s13676-014-0045-5.
URL https://www.sciencedirect.com/science/article/pii/S2192437620301114

[5] R. Ansorge, What does the entropy condition mean in traffic flow theory?, Transportation Research Part B 24 (2) (1990) 133–143. doi:10.1016/0191-2615(90)90024-S.

[6] A. Bressan, Hyperbolic systems of conservation laws, Vol. 20 of Graduate Studies in Mathematics, Oxford Lecture Series in Mathematics and its Applications, 2000.

[7] H. Holden, N. H. Risebro, Front tracking for hyperbolic conservation laws, Vol. 152, Applied Mathematical Sciences, Springer-Verlag, New York, 2002.

[8] P. D. Lax, Nonlinear hyperbolic equations, Comm. Pure Appl. Math. 6 (1953) 231–258.

[9] G. Newell, A simplified theory of kinematic waves in highway traffic, part i: General theory, Transportation Research Part B: Methodological 27 (4) (1993) 281–287. doi:https://doi.org/10.1016/0191-2615(93)

90038-C.
URL https://www.sciencedirect.com/science/article/pii/0191261593900 38C

[10] G. Newell, A simplified theory of kinematic waves in highway traffic, part ii: Queueing at freeway bottlenecks, Transportation Research Part B: Methodological 27 (4) (1993) 289–303. doi:https://doi.org/10.1016/0191-2615(93)90039-D.
URL https://www.sciencedirect.com/science/article/pii/0191261593900 39D

[11] G. Newell, A simplified theory of kinematic waves in highway traffic, part iii: Multi-destination flows, Transportation Research Part B: Methodological 27 (4) (1993) 305–313. doi:https://doi.org/10.1016/0191-2615(93)90040-H.
URL https://www.sciencedirect.com/science/article/pii/0191261593900 40H

[12] C. F. Daganzo, A variational formulation of kinematic waves: basic theory and complex boundary conditions, Transportation Research Part B: Methodological 39 (2) (2005) 187–196. doi:https://doi.org/10.1016/j.trb.2004.04.003.
URL https://www.sciencedirect.com/science/article/pii/S0191261504000487

[13] C. F. Daganzo, On the variational theory of traffic flow: Well-posedness, duality and applications, Netw. Heter. Med. 1 (2006) 601–619.

[14] K. T. Joseph, G. D. V. Godwa, Explicit formula for the solution of convex conservation laws with boundary condition, Duke Mathematical Journal 62 (2) (1991) 401–416.

[15] K. T. Joseph, G. D. V. Godwa, Solution of convex conservation laws in a strip, Proc. of the Indian Academy of Sciences-Mathematical Sciences 102 (1) (1992) 29–47.

[16] C. G. Claudel, A. M. Bayen, Lax–hopf based incorporation of internal boundary conditions into hamilton–jacobi equation. part i: Theory, IEEE Transactions on Automatic Control 55 (5) (2010) 1142–1157. doi:10.1109/TAC.2010.2041976.

[17] C. G. Claudel, A. M. Bayen, Lax–hopf based incorporation of internal boundary conditions into hamilton-jacobi equation. part ii: Computational methods, IEEE Transactions on Automatic Control 55 (5) (2010) 1158–1174. doi:10.1109/TAC.2010.2045439.

[18] P.-E. Mazaré, A. H. Dehwah, C. G. Claudel, A. M. Bayen, Analytical and grid-free solutions to the lighthill–whitham–richards traffic flow model, Transportation Research Part B: Methodological 45 (10) (2011) 1727–1748. doi:https://doi.org/10.1016/j.trb.2011.07.004.
URL https://www.sciencedirect.com/science/article/pii/S0191261511001044

[19] M. D. Simoni, C. G. Claudel, A fast lax–hopf algorithm to solve the lighthill–whitham–richards traffic flow model on networks, Transportation Science 54 (6). doi:10.1287/trsc.2019.0951.

[20] Y. Lu, S. Wong, M. Zhang, C.-W. Shu, W. Chen, Explicit construction of entropy solutions for the lighthill–whitham–richards traffic flow model with a piecewise quadratic flow–density relationship, Transportation Research Part B: Methodological 42 (4) (2008) 355–372. doi:https://doi.org/10.1016/j.trb.2007.08.004.
URL https://www.sciencedirect.com/science/article/pii/S0191261507000781

[21] S. C. Wong, G. C. K. Wong, An analytical shock-fitting algorithm for lwr kinematic wave model embedded with linear speed–density relationship, Transportation Research Part B: Methodological 36 (8) (2002) 683–706. doi:https://doi.org/10.1016/S0191-2615(01)00023-6.

URL https://www.sciencedirect.com/science/article/pii/S0191261501000236

[22] S. K. Godunov, A difference method for numerical calculation of discontinuous solutions of the equations of hydrodynamics, Matematicheskii Sbornik 47 (3) (1959) 271–306.

[23] R. J. LeVeque, Numerical Methods for Conservation Laws, Birkhauser Verlag, Basel, Switzerland, 1990.

[24] C. F. Daganzo, The cell transmission model: A dynamic representation of highway traffic consistent with the hydrodynamic theory, Transportation Research Part B: Methodological 28 (4) (1994) 269–287. doi:10.1016/0191-2615(94)90002-7.

[25] C. F. Daganzo, The cell transmission model, part ii: network traffic, Transportation Research Part B: Methodological 29 (2) (1995) 79–93. doi:10.1016/0191-2615(94)00022-R.

[26] I. Yperman, The Link Transmission Model for dynamic network loading, PhD Thesis, Katholieke Universiteit Leuven, Belgium, 2007.

[27] H. Holden, N. H. Risebro, A mathematical model of traffic flow on a network of unidirectional roads, SIAM J. Math. Anal. 26 (4) (1995) 999–1017. doi:10.1137/S0036141093243289.

[28] G. M. Coclite, M. Garavello, B. Piccoli, Traffic flow on a road network, SIAM J. Math. Anal. 36 (6) (2005) 1862–1886. doi:10.1137/S0036141004402683.

[29] M. Garavello, B. Piccoli, Traffic Flow on Networks. Conservation Laws Models, AIMS Series on Applied Mathematics, Springfield, MO, USA, 2006.

[30] G. Tilg, L. Ambühl, S. Batista, M. Menendez, F. Busch, On the application of variational theory to urban networks, Transportation Research Part B: Methodological 150 (2021) 435–456.

doi:https://doi.org/10.1016/j.trb.2021.06.019.
URL https://www.sciencedirect.com/science/article/pii/S0191261521001302

[31] A. K. Ziliaskopoulos, S. T. Waller, Y. Li, M. Byram, Large-scale dynamic traffic assignment: implementation issues and computational analysis, Journal of Transportation Engineering 130 (5) (2004) 585–593.

[32] R. L. Hughes, A continuum theory for the flow of pedestrians, Transportation Research Part B: Methodological 36 (6) (2002) 507–535. doi:10.1016/S0191-2615(01)00015-7.

[33] F. D. Rossa, C. D'Angelo, A. Quarteroni, A distributed model of traffic flows on extended regions, Networks & Heterogeneous Media 5 (3) (2010) 525–544.

[34] Y. Jiang, S. Wong, H. Ho, P. Zhang, R. Liu, A. Sumalee, A dynamic traffic assignment model for a continuum transportation system, Transportation Research Part B: Methodological 45 (2) (2011) 343–363. doi:10.1016/j.trb.2010.07.003.

[35] J. Du, S. Wong, C.-W. Shu, T. Xiong, M. Zhang, K. Choi, Revisiting jiang's dynamic continuum model for urban cities, Transportation Research Part B: Methodological 56 (2013) 96–119. doi:10.1016/j.trb.2013.07.001.

[36] Y.-Q. Jiang, P.-J. Ma, S.-G. Zhou, Macroscopic modeling approach to estimate traffic-related emissions in urban areas, Transportation Research Part D: Transport and Environment 60 (2018) 41–55, special Issue on Traffic Modeling for Low-Emission Transport. doi:https://doi.org/10.1016/j.trd.2015.10.022.
URL https://www.sciencedirect.com/science/article/pii/S1361920915001996

[37] R. Aghamohammadi, J. A. Laval, Dynamic traffic assignment using the macroscopic fundamental diagram: A review of vehicular and pedestrian

flow models, Transportation Research Part B: Methodological 137 (2020) 99–118. doi:10.1016/j.trb.2018.10.017.

[38] S. Mollier, M. L. Delle Monache, C. C. de Wit, B. Seibold, Two-dimensional macroscopic model for large scale traffic networks, Transportation Research Part B: Methodological 122 (2019) 309 – 326. doi:10.1016/j.trb.2019.02.016.

[39] Z. Y. Lin, S. C. Wong, P. Zhang, Y. Q. Jiang, K. Choi, Y. C. Du, A predictive continuum dynamic user-optimal model for a polycentric urban city, Transportmetrica B: Transport Dynamics 5 (3) (2017) 228–247. doi:10.1080/21680566.2016.1163297.

[40] S. Mollier, M. L. Delle Monache, C. Canudas-de-Wit, A step towards a multidirectional 2d model for large scale traffic networks, in: TRB 2019 - 98th Annual Meeting Transportation Research Board, Washington D.C., USA, Jan. 2019, pp. 1–7. doi:hal-01948466.

[41] R. Aghamohammadi, J. A. Laval, A continuum model for cities based on the macroscopic fundamental diagram: a semi-lagrangian solution method, Transportation Research Procedia 38 (2019) 380–400. doi:10.1016/j.trpro.2019.05.021.

[42] L. Tumash, C. C. de Wit, M. L. D. Monache, Boundary control for multi-directional traffic on urban networks, Submitted to 2021 IEEE 60th Conference on Decision and Control (CDC), December 2021, Austin, Texas, USA.
URL https://hal.archives-ouvertes.fr/hal-03182546

[43] D. Nikitin, C. C. de Wit, P. Frasca, A continuation method for large-scale modeling and control: from odes to pde, a round trip, arXiv:2101.10060.

[44] D. Serre, Systems of Conservation Laws I: Hyperbolicities, Entropies, Shock Waves, Cambridge University Press, Cambridge, 1999.

[45] R. Courant, K. Friedrichs, H. Lewy, On the partial difference equations of mathematical physics, IBM Journal of Research and Development 11 (2) (1967) 215–234. doi:10.1147/rd.112.0215.

[46] R. Courant, E. Isaacson, M. Rees, On the solution of nonlinear hyperbolic differential equations by finite differences, Communications on Pure and Applied Math. 5 (1952) 243–255. doi:10.1002/cpa.3160050303.

[47] Zhou Wang, A. C. Bovik, H. R. Sheikh, E. P. Simoncelli, Image quality assessment: from error visibility to structural similarity, IEEE Transactions on Image Processing 13 (4) (June 2004) 600–612. doi:10.1109/TIP.2003.819861.

[48] M. Rodriguez-Vega, Optimal sensor placement and density estimation in large-scale traffic networks, PhD Thesis, University Grenoble Alpes, 2021.

[49] C. C. de Wit, F. Morbidi, L. L. Ojeda, A. Y. Kibangou, I. Bellicot, P. Bellemain, Grenoble traffic lab: An experimental platform for advanced traffic monitoring and forecasting [applications of control], IEEE Control Systems Magazine 35 (3) (2015) 23–39. doi:10.1109/MCS.2015.2406657.

[50] M. Rodriguez-Vega, C. Canudas-de-Wit, H. Fourati, Urban network traffic state estimation using a data-based approach, in: CTS 2021 - 16$^{\text{th}}$ IFAC Symposium on Control in Transportation Systems, Lille, France, June 2021. doi:hal-03171255.